

# 非線性三維河口污染物擴散模式之研究—速度/渦度法 (1/3)

## Nonlinear 3D Mathematical Modeling of Pollutant Transport in Estuaries by the Method of Velocity-Vorticity Formulation(1/3)

計畫編號：NSC-88-2611-E-002-030

執行期間：87年8月1日至88年7月31日

主持人：楊德良 國立台灣大學土木系教授及

國立台灣大學水工試驗所研究員

### 一、中文摘要（關鍵字：河口水理、

污染物傳輸與擴散、速度-渦度法、邊界元素法，有限元素法）

本研究目的，在於以數值模式模擬非線性三維河口污染物擴散之物理現象。由於物理包涵的層面廣泛，因此在盡量以數值模式呈現實際的現象，又必須顧及數值計算上的限制，所以在模式上儘量減低處理非線性方程式，因而我們在水理模式採用了以速度—渦度觀念，使得在處理速度分佈，祇為分離之線性 Poisson 方程式，而在渦度場方面，則為傳統之傳輸—擴散—反應方程式。為了達到降低維度，我們同時使用了邊界元素法 (BEM) 及有限元素法 (FEM)，以求解渦度、溫度、鹽度及污染物之傳輸—擴散—反應方程式。因此本研究重點，即著重於線性 Poisson 方程式之邊界元素及有限元素模式的建立與應用及速度—渦度觀念之可行性。

本文利用速度 (Velocity) - 渦度 (Vorticity) 法搭配有限元素法 (Finite element method)，邊界元素法 (Boundary element method) 及二階朗吉庫特法 (Runge-Kutta method) 求解三維慣性座標和非慣性座標不可壓縮黏性流場，文中以簡單之三維箱型穴室流 (Cavity flow) 作為驗證程式的依據。在驗證過程中，對奈維爾-司徒克斯 (Navier-Stokes) 方程式在中低雷諾茲數流場作分析，以瞭解流場變化和渦度變化的關係。由驗證的結果中發現邊界的黏滯力將

導致渦度的改變，而渦度會擴散至整個流場中，帶動整個流場變化，造成速度改變，而流場速度變化又相繼改變渦度，如此相互反制影響。

本文為在模式建立之初，分別以慣性座標與非慣性座標之流況下，模擬流場隨著雷諾茲數的改變，及在加入向心力項和科氏力項之後，對流場的影響更趨於複雜。在模擬的流場採用雷諾茲數為 20、100、200、600、800、1300，當流場之非線性項之作用逐漸增強時，速度梯度變化劇烈之處，本模式亦能反應流場狀況且計算收斂性強，這是因為速度-渦度法是直接計算渦度，而渦度是速度的一次微分，所以能以較少的網格數，來表現速度的劇烈變化。在非慣性座標的驗證，我們取 Rossby 數為 0.1 之模擬流況。初步驗證的結果，和運動方程式所表現的運動行為是相吻合的。為了初步模擬有密度層變污染物傳輸的可行性，本模式取福祿數  $Fr=0.05$ ，結果發現速度場及渦度場變化相當大，而溫度場及濃度場之改變則不如速度及渦度來的明顯。這些現象都滿足速度、溫度與污染物擴散的物理現象。

英文摘要 ((Keywords : Estuary hydrodynamics, Pollutant advection-diffusion, Velocity-vorticity method, Boundary element method ,Finite element method )

The main purpose of present study aims at the establishment of a mathematical model for predicting the pollutant transport in a nonlinear 3D estuary. To reduce the handling of nonlinear partial differential equations, the concept of velocity-vorticity formulation is adopted to model the estuary hydrodynamics. Thus the governing equations for the velocity field are deduced to the linear Poisson equations. To further lower the dimension, the BEM is again applied to solve the velocity Poisson equation. The distribution of pollutant, temperature, as well as salinity are all solved by the FEM algorithms as well as the the feasibility of the concept of velocity-vorticity formulation.

In this study, we use the velocity-vorticity method, in combination with finite element method, boundary element method and Runge-Kutta method to solve the three-dimensional inertial and non-inertial unsteady incompressible viscous flows. The correctness of the model is verified by a simple driven cavity flow by comparing with existing literature.

As far as flow verification is concerned, we analyze the flows satisfying the Navier-Stokes equations with low Reynolds numbers. In computation, one can understand the relation between the change of flow velocity and

vorticity. By the process of verification, we know the fact that the viscous force on the boundary induces the generation of the vorticity, and interactively the vorticity would diffuse into the whole flows, and cause the variation of the flows. However the variation of the flows also will change the vorticity. Finally, they are influenced and coupled each other.

We have established the Navier-Stokes equations for both the inertial and non-inertial coordinate systems. The Reynolds numbers were chosen to be 20,100,200,600, and 1300 to reflect the strong influences of nonlinear phenomenon. Even using very coarse grids, the models render good results for both with and without considering the effect of coriolis force. We also calculate the role of density stratification for Froude number equal to  $Fr=0.05$  and investigate the importance of density influence to the estuaries. The pollutant transport for the associated flow field is also studied and shows promising progress. The variations of velocity and vorticity fields are stronger than those of temperature and pollutant concentration. These

characteristics are all correspondent to the mechanisms of transports of velocity, temperature and pollutant concentration.

## 二、計畫原由與目的

台灣地區地狹人稠四面環海，土地利用的限制及環境保護意識的抬頭，促使發展的觸角伸向河流及海洋。因此，河口及沿海之開發日益頻繁，人口快速的成長及高科技工業之發展，對水域之水質與環境造成負面之影響，水質規畫與管理之工作成為重要的課題，然而，河口及沿海水域之污染物傳輸與擴散機制深受河川流量及水質、海洋潮汐、洋流運動、風力、地球自轉之科氏力、海水密度層變及河口與海岸地形等因素所影響。欲瞭解河口及沿海水域複雜污染物對流、擴散與反應現象，水理與水質數值模擬應是最佳之分析方法。

在國科會的資助下，「三維河口污染物擴散模式之研究」以建立三維時變之線性水理及水質數值模式，Young and Wang (1994), Young and Wang (1995)，楊德良、何柏釗 (1996) , Young and Lin(1994), Young and Lin (1996)，透過數值模擬測試，已可明瞭河口及沿海大尺度之淺水流場受海洋潮汐作用產生之週期運動、受科氏力影響之愛克曼螺旋機制、風剪力拖曳效應及海水密度層變之影響。模式應用邊界元素法（邊界積分法）以解決速度-渦度法中推求邊界條件不精確之難處，並降低數值擴散及數值延散之產生。

本計畫擬繼續探討國科會資助下之「非線性三維河口污染物擴散模式之研究」，楊德良、楊勝凱 (1997)，楊德良等 (1998)，我們已成功的發展一

套利用邊界積分法及有限元素法來解決非定常性之污染物的傳輸擴散模式，對於降低維度與減少數值擴散與數值延散，均有良好之結果。對於河口污染物擴散之研究，將可更上一層樓。研究方向將分三個階段進行，第一階段進行沒有密度層變與有密度層變之非線性水理與污染物邊界積分數值模式之建立與比較，以瞭解慣性力與水平擴散相對於水理之影響。第二階段則著重有密度層變之非線性三維河口污染物之擴散模式研究，並了解各項參數對於模擬結果之影響，以利找出最佳組合，符合實際水理條件，最後階段則著重能以現場資料，尤其是淡水河口為例，探討模式應用於實際例子之可行性。

## 三、研究方法

### 3-1 水理模式

本研究為非線性極強之廣義 Navier-Stokes 方程式及連續方程式，為避開處理壓力及降低非線性與希望達成分割(decoupling)而有利於平行計算 (parallel computing)，今以速度渦度法 (velocity-vorticity method) 來求解均值 (即沒有密度層變) 之河口水理。其基本方程式為

$$\nabla^2 \bar{u} = -\bar{\nabla} \times \bar{\omega} \quad (1)$$

$$\frac{\partial \bar{\omega}}{\partial t} + \bar{u} \cdot \bar{\nabla} \bar{\omega} = \nu \bar{\nabla}^2 \bar{\omega} + (\bar{\omega} + f \bar{k}) \cdot \bar{\nabla} \bar{u} \quad (2)$$

式中  $f = 2\Omega \sin \theta$ ,  $\bar{\omega} = \bar{\nabla} \times \bar{u}$

### 3-2 污染物傳輸模式

描述污染物傳輸模式，一般以所謂之傳輸 (advection)、擴散 (diffusion) 及反應 (reaction) 方程式為之，即

$$\frac{\partial \bar{C}}{\partial t} + \bar{u} \cdot \nabla^2 \bar{C} = k_c \nabla^2 \bar{C} + \bar{S}_c(\bar{C}, \bar{x}, t) \quad (3)$$

我們以所發展之有限元素法 (FEM) 來處理渦度、溫度、鹽度及污染物之傳輸擴散，及反應方程式。因為在第二階段有密度層變 (density stratification) 之計畫中，吾人只要在第 (2) 式中增加因密度而增加之渦度即可。

$$\frac{\partial \bar{\omega}}{\partial t} + \bar{u} \cdot \nabla \bar{\omega} = \nu \nabla^2 \bar{\omega} + (\bar{\omega} + f\bar{k}) \cdot \nabla \bar{u} + \nabla \times \left( -g \frac{\rho - \rho_0}{\rho} \bar{k} \right) \quad (4)$$

及狀態方程式

$$\rho = \rho(T, S, \bar{C}) \quad (5)$$

及溫度方程式

$$\frac{\partial T}{\partial t} + \bar{u} \cdot \nabla T = k_T \nabla^2 T + S_T(T, \bar{x}, t) \quad (6)$$

及鹽度方程式

$$\frac{\partial S}{\partial t} + \bar{u} \cdot \nabla S = k_S \nabla^2 S + S_S(S, \bar{x}, t) \quad (7)$$

### 3-3 數值模擬結果

本文為利用速度-渦度法之觀念，以求解速度場及渦度場。為考慮龐大之計算量與流場之複雜性，以幾何形狀較為簡單之三維穴室流場為例子。在速度場求解，係以邊界元素法 (BEM) 為主軸，分別求解  $u$  及  $v$  與  $w$  之速度分向。而在渦度場之解法，則是利用目前發展之有限元素法 (FEM)，求解渦度之傳輸與擴散過程。模擬的結果由驗證、比較到初步結果，將說明如下。模擬雷諾茲數 200 之  $v$  方向速度及  $w$  方向速度的圖中，即圖 1 和圖 2，可看出速度  $v$  仍為一規則流場，整個流場為一個大渦漩所環繞，其渦心偏向右上角落，此可能為受上方  $u$  方向之拖曳速度及邊界不

滑動的影響造成，其速度由渦心向外逐漸增大且向下傳遞。而  $w$  方向仍為對稱流場，流場的變化尚不顯著。此雷諾茲數之渦度場，在  $z$  方向與  $x$  方向仍呈現對稱流況，渦度亦集中在邊界附近，尤其是左上及右上角落，此可由圖 3 及圖 4 中得知。當雷諾茲數為 600 時，流況與雷諾茲數 200 的流況有所差異。圖 5 與圖 6 所示的速度圖，同樣  $v$  方向之速度場，其渦漩擴大至整個流場， $w$  方向速度場亦因雷諾茲數的增加，而使渦漩的形成更為明顯。在圖 7 與圖 8 中，渦度場的分佈，不管是在  $z$  或  $x$  方向，均向內部逐漸擴散傳遞，且其強度隨之增加。當雷諾茲數增加到 1300 時， $v$  方向速度場之渦漩更為緊密，在  $w$  方向渦漩的分佈不再是那麼均勻，四個邊角的渦漩有逐漸擴大之勢，呈現之流況也有所不同。在渦度場中，渦度值的分佈可看出已非如前幾個的例子，對稱分佈於流場中，顯示流場隨雷諾茲數增加，漸漸趨向非對稱之流況。然因所取的網格過於粗糙，於速度場中並不明顯，但於渦度場中則可略窺究竟。這些模擬結果則分別示於圖 9、圖 10、圖 11 及圖 12。

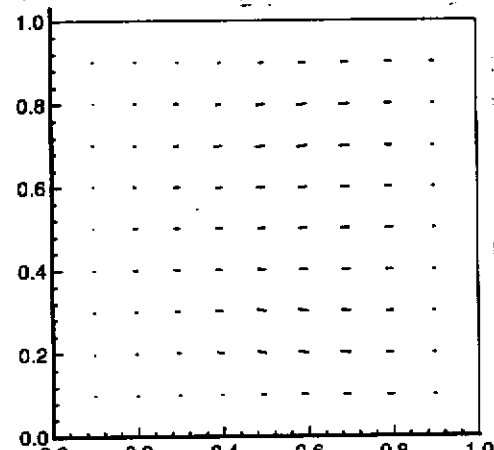


圖 1：雷諾茲數 200 在  $z=0.5$  之速度場  $u$  和  $v$  分佈圖

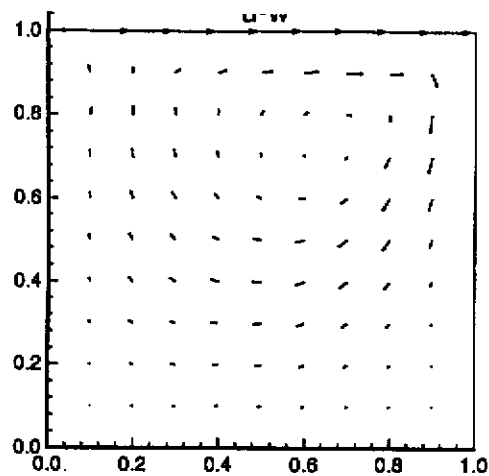


圖 2：雷諾茲數 200 在  $y=0.5$  之速度

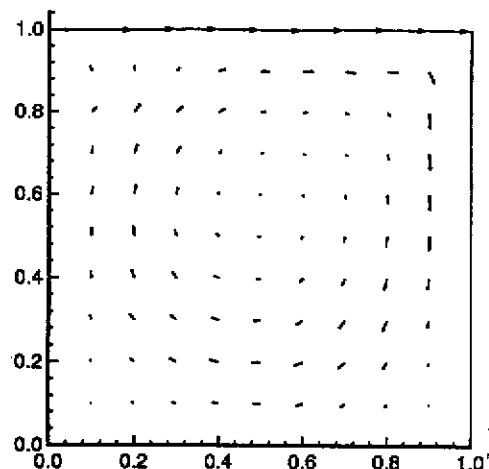


圖 5：雷諾茲數 600 在  $y=0.5$  之速度分佈圖

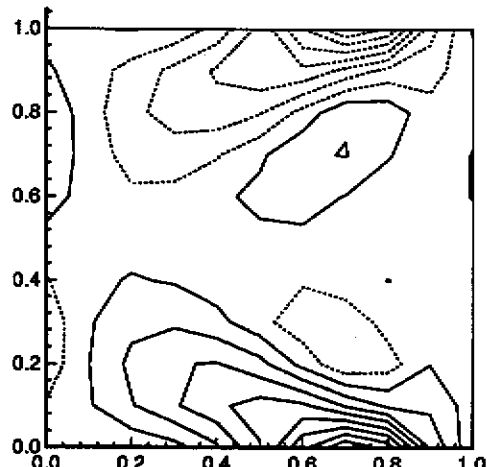


圖 3：雷諾茲數 200 在  $z=0.5$  之  
渦度  $\xi$  分佈圖

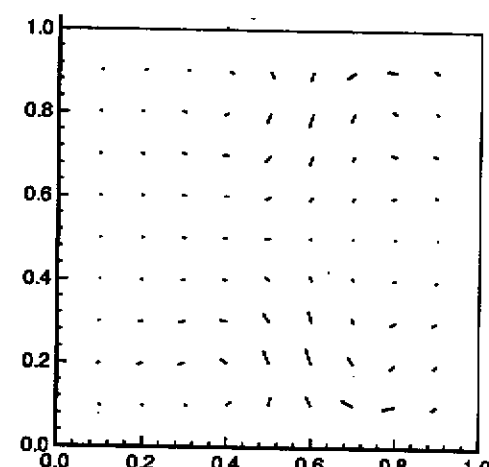


圖 6：雷諾茲數 600 在  $z=0.5$ ，  
之速度分佈比較圖

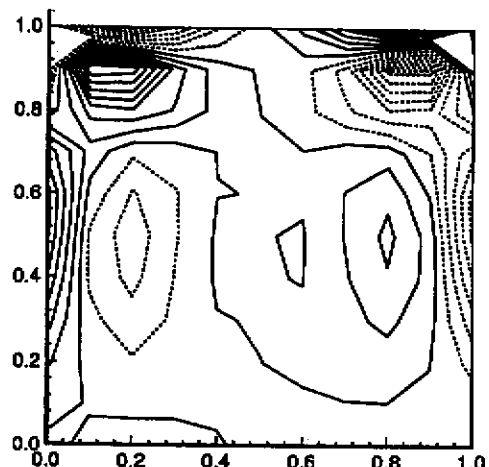


圖 4：雷諾茲數 200 在  $x=0.5$ ，  
之渦度  $\xi$  分佈圖

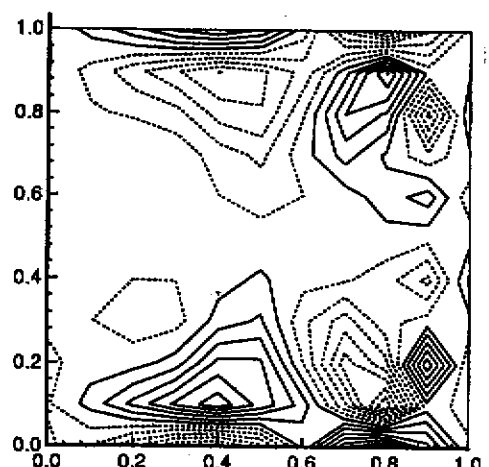


圖 7：雷諾數 600 在  $z=0.5$  之渦度場  
 $\xi$  分佈圖

以上在慣性座標下之模擬結果，由渦度場  $\zeta$  和速度場，可明顯了解，流場內逐漸形成大小渦旋的離形。而由渦度場中渦度值分佈狀況，了解當流場加入非慣性的影響考慮之後，將使得模擬的結果更為複雜，相對的，也更接近實際流況的物理現象。

在非慣性座標的流場，先假設向心力沒有影響，而流場的邊界條件和先前一樣，只是方程式中因沿負  $z$  軸旋轉， $\bar{\Omega} = -\bar{k}$ ，造成科氏力影響渦度的變化。若和無科氏力影響的流場比較，整個流場是做一螺旋轉動。

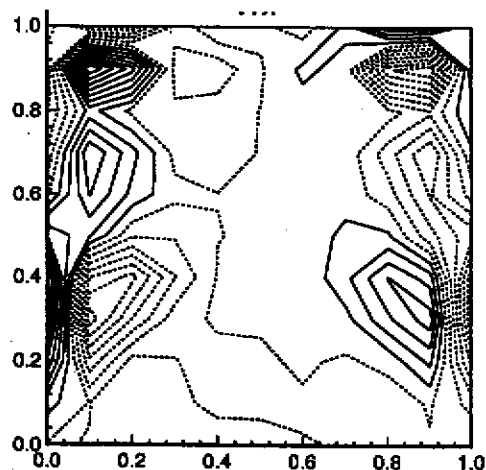


圖 8：雷諾數 600 在  $x=0.5$  之渦度場  $\zeta$  分佈圖

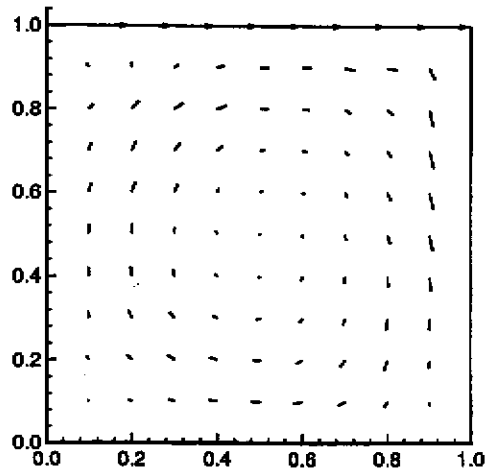


圖 9：雷諾數 1300 在  $y=0.5$  之速度場分佈圖

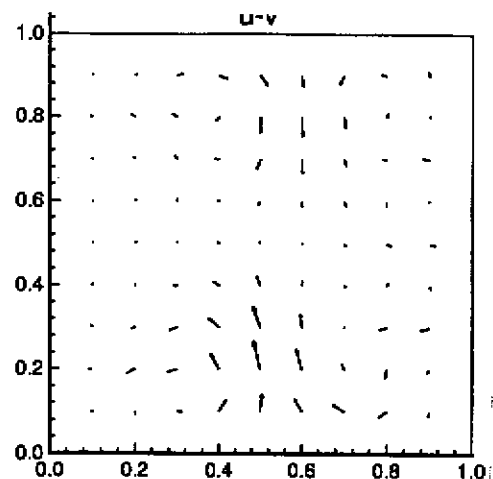


圖 10：雷諾數 1300，在  $z=0.5$  之速度場分佈圖

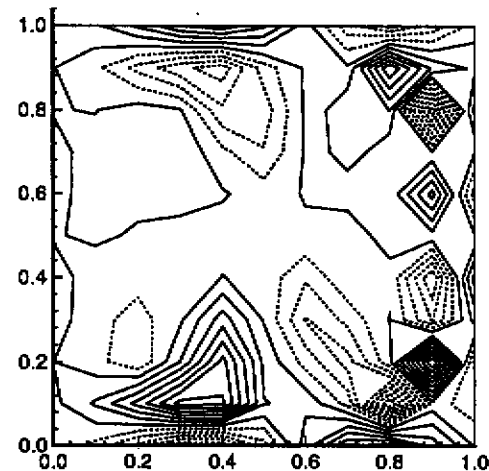


圖 11：雷諾數 1300，在  $z=0.5$  之渦度場  $\zeta$  分佈圖

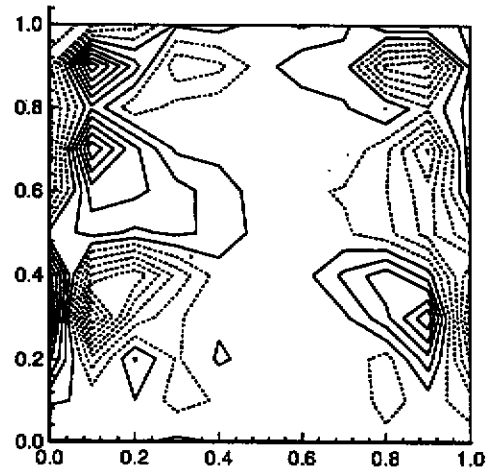


圖 12：雷諾數 1300，在  $x=0.5$  之渦度場  $\zeta$  分佈圖

在三維有密度層變河口污染物擴散的模式中，渦度方程式中只需增加因密度層變所造成渦度變化。而溫度方程式，即(6)式的邊界條件，為了充分模擬河口的溫度變化，本文採用水面與空氣交界處，即 $z=1$ 的平面其無因次的溫度較低，並當作0。而污染物擴散方程式的邊界條件，為了了解濃度的分佈情況，僅在 $z=1$ 、 $x=0.5$ 、 $y=0.5$ 之處其只為1，其餘邊界為0。

在密度層變的考慮下，由圖13可看出流場在 $y=0.5$ 的平面上已自成上下兩區。而由圖14中可之，除了因旋轉方向相反所造成的速度場轉向正y軸以外，整個流場的變動快速傳遞到流場的每個角落，且在低雷諾茲數之密度層變流況下，呈現對稱流況。溫度場可由圖15可看出，溫度分佈由上方逐漸往下傳遞，而由圖16可知，濃度也由一點逐漸擴散至流場中。

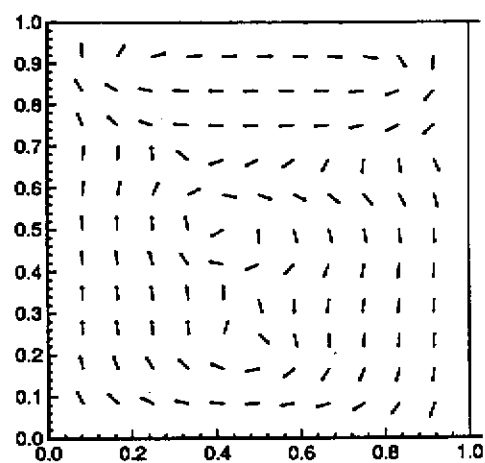


圖 13：雷諾數 20·Rossby 數為 0.1 Froude 數為 0.05 在  $y=0.5$  之速度場  $u$  和  $w$  分佈圖

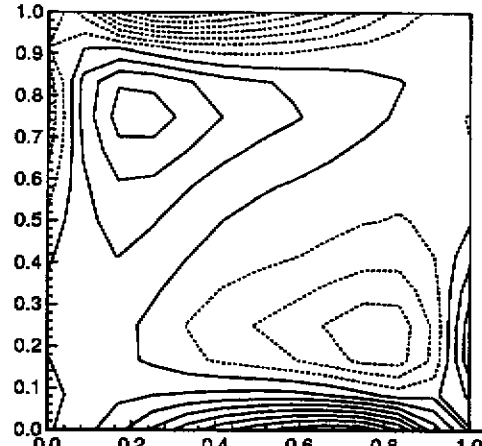


圖 14：雷諾數 20·Rossby 數為 0.1 Froude 數為 0.05 在  $z=0.5$  之渦度場  $\zeta$  分佈圖

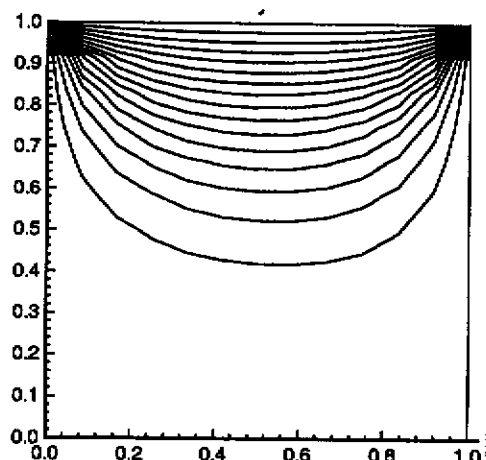


圖 15：雷諾數 20·Rossby 數為 0.1 Froude 數為 0.05 在  $y=0.5$  之溫度場分佈圖

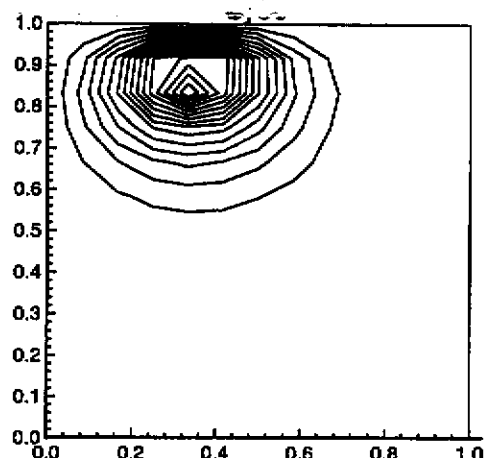


圖 16：雷諾數 20·Rossby 數為 0.1 Froude 數為 0.05 在  $z=0.5$  之濃度場分佈圖

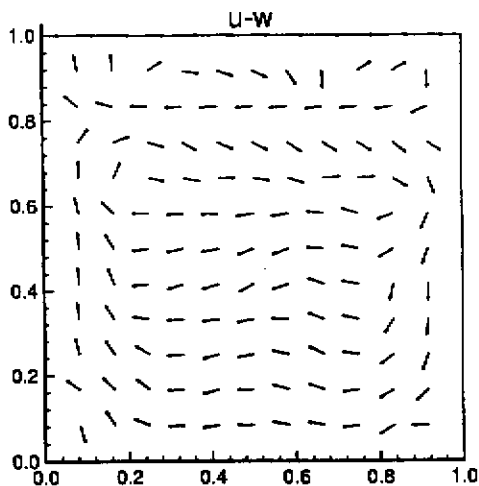


圖 17: 雷諾數 100, Rossby 數 0.1  
Froude 數為 0.05 在  $z=0.5$   
之速度場  $u$  和  $w$  分佈圖

在同樣非線性密度層變的條件下，雷諾茲數 100 的流況遠比雷諾茲數 20 的流況變動更大。在速度場中， $x$  方向的速度向量受到邊界影響擴大，由原先的大渦旋逐漸的形成一個、兩個的渦旋分佈在流場中，尤其位於邊界角落附近，而在圖 17 中  $y$  方向的速度向量圖中邊界角落隱約形成。流場速度受科氏力及向心力的影響仍明顯，因此，在圖 18 的渦度分佈圖中，可見一斑。溫度與濃度隨著時間的進行、速度的變化，越往下擴散，此可由圖 19 及圖 20 中清楚顯示。

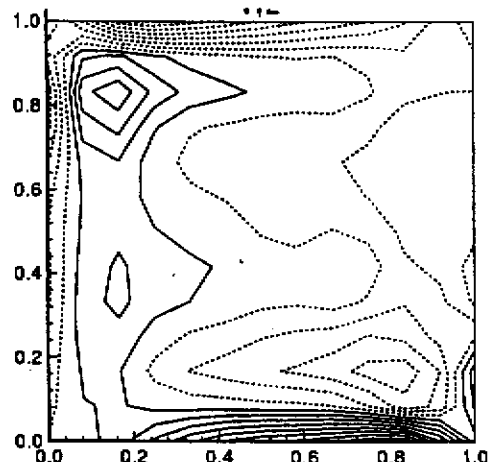


圖 18: 雷諾數 100, Rossby 數 0.1  
Froude 數為 0.05 在  $z=0.5$   
之渦度場  $\zeta$  分佈圖

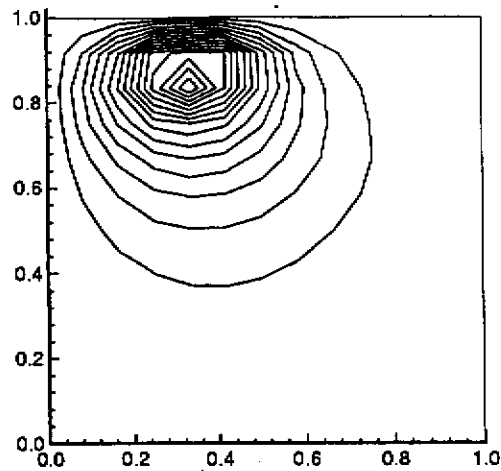


圖 19: 雷諾數 100, Rossby 數 0.1  
Froude 數為 0.05 在  $y=0.5$   
之濃度場分佈圖

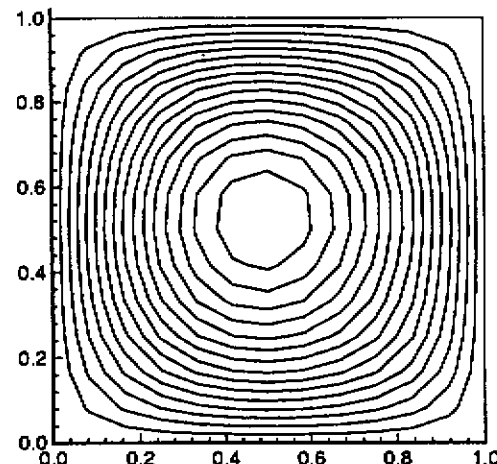


圖 20: 雷諾數 100, Rossby 數 0.1  
Froude 數為 0.05 在  $z=0.5$   
之溫度場分佈圖

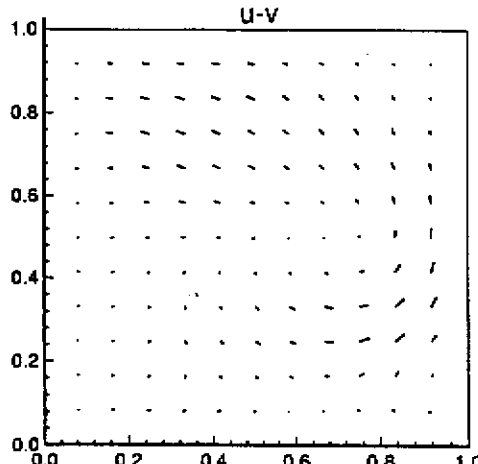


圖 21: 雷諾數 200, Rossby 數 0.1  
Froude 數為 0.05 在  $z=0.5$   
之速度場  $u$  和  $v$  分佈圖

當雷諾茲數為 200 時，在  $z$  方向速度分佈圖中，即圖 21，其流場相較之前較低雷諾數的流況，渦旋更為具體，且其渦心略微偏右。相對於渦度場而言，由圖 22 中了解渦度值變化集中於右中下部分，負渦度值亦逐漸往中心傳遞。雖然，速度場和渦度場的變化頗大，但溫度及濃度的變化就不如速度與渦度來的明顯，仍以一定速度向下及往四周傳遞及擴散，如圖 23、圖 24。

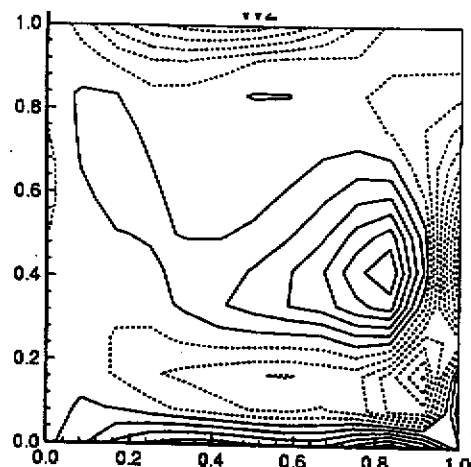


圖 22：雷諾數 200，Rossby 數 0.1 Froude 數為 0.05 在  $z=0.5$  之渦度場  $\zeta$  分佈圖

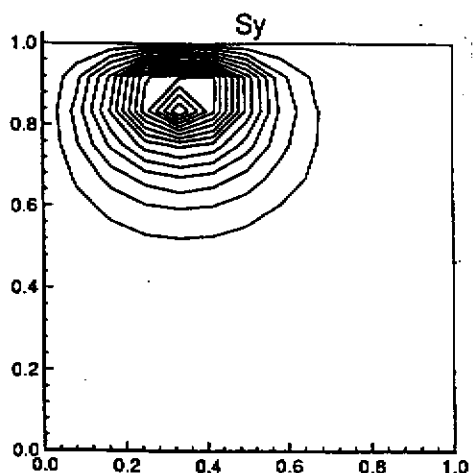


圖 23：雷諾數 200，Rossby 數 0.1 Froude 數為 0.05 在  $y=0.5$  之濃度場分佈圖

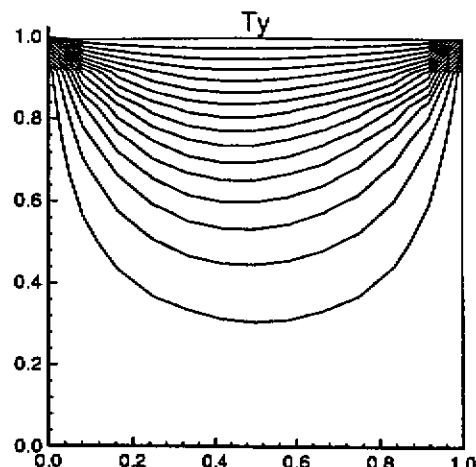


圖 24：雷諾數 200，Rossby 數 0.1 Froude 數為 0.05 在  $y=0.5$  之溫度場分佈圖

#### 四、結論與建議

1. 本研究利用邊界元素法求解速度場之 Poisson 方程式，利用有限元素法及二階朗吉庫特法求解渦度、溫度、污染物濃度場之傳輸-擴散-反應方程式，發現是一個解決非線性三維河口污染物擴散研究的可行方法。
2. 文中對控制參數，如雷諾茲數代表非線性，福祿數代表密度層變的影響，Rossby 數代表 Coriolis 力的影響作了初步的探討。即使較粗網格的限制下，其結果與三維非線性河口的水理現象是吻合的。
3. 為了探討更有效率的數值方法，本研究擬採用其他數值方法，如對偶互換邊界元素法 (Dual Reciprocity BEM) 及有限差分法或完全有限元素法等，繼續研究改進，希望在計畫結束時，能有更好的研究成果。

#### 參考文獻

1. Young,D.L., and Wang,Y.F.,1994,3D Mathematical Modelling of Pollutant Transport in Estuaries(I),行政院國科會專題計畫成果報告，中華民國 83 年 12 月。
2. Young,D.Y.,and Wang,Y.F.,1995,3D Mathematical Modelling of Pollutant Transport in Estuaries (II),行政院國科會專題計畫成果報告，中華民國 84 年 12 月。
3. 楊德良、何柏鉤，1996，三維河口污染物擴散模式之研究（三），行政院國科會專題計畫成果報告，中華民國 85 年 10 月。
4. Young,D.Y., and Lin,J.Y. , 1994, Numerical Visualization of Three Dimensional Flow Fields and Pollutant Transport,行政院國科會大學生暑期參與專題研究計畫成果報告，中華民國 83 年 12 月。
5. Young,D.Y., and Lin,J.Y., 1996, Numerical Visualization of Three Dimensional Pollutant Transport in Estuaries,行政院國科會大學生暑期參與專題研究計畫成果報告，中華民國 85 年 2 月。
6. 楊德良，楊勝凱，1997，非線性三維河口污染物擴散模式之研究（一），行政院國科會專題計畫成果報告，1997 年 11 月。
7. 楊德良等, 1998, 非線性三維河口污染物擴散模式之研究（二），行政院國家科學委員會專題計畫成果報告, 1998 年 12 月。

B5. 廖清標，楊德良，盧泰成，吳銘順，1999，“以速度-湍度列序法求解三維不可壓縮流”，第六屆計算流體力學學術研討會論文集，台東，pp.239-246。

## 以速度一渦度列式法求解三維不可壓縮流

## VELOCITY - VORTICITY FORMULATION FOR 3D INCOMPRESSIBLE FLOW

廖清標/逢甲大學水利工程學系副教授

楊德良/台灣大學土木工程學系教授

盧泰成/逢甲大學土木及水利工程研究所

吳銘順/逢甲大學土木及水利工程研究所

### 摘要

本文利用速度一渦度列式法採用有限差分法來求解不可壓縮、粘性流體之運動，以三維穴流及三維後向階梯流流場為例，分別進行數值計算工作。數值模式以顯示Adams-Basforth法來求解Helmholtz vorticity transport equation；對速度之Poisson方程式則利用快速傅利葉轉換(FFT)法直接解出。配合MAC交錯網格系統，在求解過程不需要渦度的邊界條件，且速度與渦度在求解過程中可以不必疊代程序，數值解的精確度不論在時間或空間上都具二階精確度。初步研究結果經與前人研究之實驗及數模比較，顯示本文數值模式相當成功。

**關鍵詞：**速度一渦度列式法，三維流，穴流，後向階梯流。

### ABSTRACT

The motion of incompressible and viscous fluid in a three-dimensional square cavity and three-dimensional backward-facing step are solved by the finite difference method using the velocity-vorticity formulation.

For the calculation of Helmholtz vorticity transport equation, explicit Adams-Basforth scheme is proposed. The Fast Fourier Transform (FFT) is suggested to directly solve the velocity Poisson's equation. In conjunction with staggered grid system, the boundary condition of vorticity is satisfied automatically and without any consideration.

Iteration process is not necessary in the solving process between velocity and voroticity of proposed numerical method. By the way, the numerical solution reaches second-order accuracy in both time and space. The preliminary results of this study show that the numerical method is quite successful.

**KEYWORDS:** velocity-vorticity formulation, three-dimensional flows, cavity flow, backward-facing step flow.

### 一、前言

流體中分離流的行為在流體力學上一直是受關注的研究課題，為瞭解其特有之物理意義亦吸引眾多學者投入研究，往往從較簡單之幾何形狀著手，從事相關實驗或數值計算之研究工作。分離流可定義為：鄰

近固體邊界迴流區流場，其迴流區位置以“渦流泡”之離開和再接觸而定，通常以鄰近邊界之零渦度來區分。例如：1.凸擴管流場 2.孔口流場 3.渠流越流過一階梯或薄柵 4.穴流流場 5.後向階梯流場。

每一結構流場皆有其不同的邊界條件，亦隨趨動流體和質量傳遞與動量交換亦會使流場問題更顯示不同狀況。這些流動問題為典型的初始～邊界值問題，配合流場適當的初始及邊界條件，即能求得任何時刻之流場解答。

本文研究以穴流及後向階梯流場為主軸，以數值模式測試流場穴流之流場特徵，三維穴流為上部流體受拉動，順沿邊壁於中央形成一大尺度之主漩渦生成過程中，由於邊壁剪力阻礙邊界層流內動量及邊壁折角駐壓的阻滯效應，遂在角落產生分流，生成小尺度的二次漩渦(secondary eddies)。它常見於許多工程上之應用，如土木水利工作中河川渠道、水壩、輸水管路之閘門導槽及衛生下水道之底槽等之相關應用。至於後向階梯流特徵，為入流場流向一突擴區域，會有向下角落產生分離流及在更下游處分別于上下邊界有再接觸長度之分離迴流泡產生，其間流場會隨Re數之增加而有不同變化。至於後向階梯流場猶如流經一突然擴大流場，隨入流之長寬不同流場亦會有不同變化，本文於此流場之比較採用Armaly *et. al.* (1983) 之實驗資料作用數值模擬驗證。

由頂蓋拖動之穴流流場實驗首先由 Pan and Acrivos (1967) 從事研究。數值模擬由頂蓋拖動之穴流流場問題之先鋒者為 Burgraff (1966)，很多此型之相關研究皆為二維模式 Ghia *et. al.* (1982)，但實際穴流流況則為三維流場。近年來PC硬體之快速發展促使三維流場之數值研究較為可行，如 Babu and Korpela (1994) 及 Chiang, Hwang and Sheu (1996) 等。

對於數值方法，速度一渦度法是利用渦度傳輸擴散方程式，及速度的Poisson方程式來求解流場，其主要困難在於渦度的邊界條件之處理及速度與渦度間互相關聯，必需疊代求解。利用本方法來求解流場如 Fusegi and Farouk (1986), Giannattasio and Napolitano (1996), 劉與楊 (1998) 等。

本文延伸廖等人 (1995) 所發展的二維模式推廣至三維流場，利用有限差分交錯網格(staggered grid system)，不需要渦度的邊界條件，且速度與渦度在

求解過程不須疊代程序，數值計算結果顯示本研究之數值模式相當成功。

## 二、理論模式

### 2.1 控制方程式

#### 1. 不可壓縮流 Navier-Stokes 方程式

$$\nabla \cdot \vec{u} = 0 \quad (1)$$

$$\frac{\partial \vec{u}}{\partial t} + \vec{u} \cdot \nabla \vec{u} = -\nabla p + \frac{1}{Re} \nabla^2 \vec{u} \quad (2)$$

式中  $\vec{u} = u\vec{i} + v\vec{j} + w\vec{k}$  為流體速度， $p$  為流體壓力， $\rho$  為流體密度， $Re$  為 Reynolds number， $Re = VL/\nu$ ， $V$  為特性速度， $L$  為特性長度， $\nu$  為流體運動粘滯性係數。

#### 2. 定義渦度 $\vec{\omega}$

$$\vec{\omega} = \nabla \times \vec{u} \quad (3)$$

$$\omega_1 = \frac{\partial w}{\partial y} - \frac{\partial v}{\partial z} \quad (4)$$

$$\omega_2 = \frac{\partial u}{\partial z} - \frac{\partial w}{\partial x} \quad (5)$$

$$\omega_3 = \frac{\partial v}{\partial x} - \frac{\partial u}{\partial y} \quad (6)$$

$$\vec{\omega} = \omega_1 \vec{i} + \omega_2 \vec{j} + \omega_3 \vec{k}$$

#### 3. 渾度傳輸方程式

對(2)式取旋度(curl)，可得

$$\frac{\partial \vec{\omega}}{\partial t} - \nabla \times (\vec{u} \times \vec{\omega}) = \frac{1}{Re} \nabla^2 \vec{\omega} \quad (7)$$

(7)式可進一步寫成

$$\frac{\partial \vec{\omega}}{\partial t} + \vec{u} \cdot \nabla \vec{\omega} = \vec{\omega} \cdot \nabla \vec{u} + \frac{1}{Re} \nabla^2 \vec{\omega} \quad (8)$$

我們可利用(7)式或(8)式來求解渾度。(8)式一般稱為 Helmholtz vorticity transport equation。

#### 4. 速度的 Poisson 方程式

由(4)-(6)式及(1)式，吾人可導出速度必須滿足下列的 Poisson 方程式

$$\nabla^2 u = \frac{\partial \omega_2}{\partial z} - \frac{\partial \omega_3}{\partial y} \quad (9)$$

$$\nabla^2 v = \frac{\partial \omega_3}{\partial x} - \frac{\partial \omega_1}{\partial z} \quad (10)$$

$$\nabla^2 w = \frac{\partial \omega_1}{\partial y} - \frac{\partial \omega_2}{\partial x} \quad (11)$$

所謂速度一渾度法就是利用(7)或(8)式配合(9)-(11)式來求解流場，而不由原來的 Navier-Stokes 方程式，即(1)和(2)式來求解。由於速度及渾度都是向量，在三維流場中共有 6 個變數待解，較原來問題 4 個變數要多解二條方程式，故一般很少使用這種方法來求解三維流動問題，但本文嘗試此方法來求解，在數值模式中為一大挑戰。

## 2.2 邊界條件

### 1. 固體邊界條件

不可滑動條件，即速度在固體邊界上為零。

$$\vec{u} = 0 \text{ on solid boundary} \quad (12)$$

## 2. 出流邊界條件

對於出流邊界之處理，本文採用線性對流條件，即在出流附近流體的渾度係以平均速度向下游傳遞。

$$\frac{\partial \omega}{\partial t} + V \frac{\partial \omega}{\partial x} = 0 \text{ on outflow } x = L \quad (13)$$

## 三、數值計算方法

### 3.1 渾度方程式的計算方法

利用顯式二階 Adams-Basforth 法來離散(7)式，可得

$$\frac{\omega_1^{n+1} - \omega_1^n}{\Delta t} + 1.5A^n - 0.5A^{n-1} = 0 \quad (14)$$

$$\frac{\omega_2^{n+1} - \omega_2^n}{\Delta t} + 1.5B^n - 0.5B^{n-1} = 0 \quad (15)$$

$$\frac{\omega_3^{n+1} - \omega_3^n}{\Delta t} + 1.5C^n - 0.5C^{n-1} = 0 \quad (16)$$

式中

$$A = \frac{\delta_x}{\Delta y} (v\omega_1) + \frac{\delta_z}{\Delta z} (w\omega_1) - \frac{\delta_y}{\Delta y} (\omega_2 u) - \frac{\delta_z}{\Delta z} (\omega_3 u)$$

$$- \frac{1}{Re} \left( \frac{\delta_x^2}{\Delta x^2} + \frac{\delta_y^2}{\Delta y^2} + \frac{\delta_z^2}{\Delta z^2} \right) \omega_1$$

$$B = \frac{\delta_x}{\Delta x} (u\omega_2) + \frac{\delta_z}{\Delta z} (w\omega_2) - \frac{\delta_x}{\Delta x} (\omega_1 v) - \frac{\delta_z}{\Delta z} (\omega_3 v)$$

$$- \frac{1}{Re} \left( \frac{\delta_x^2}{\Delta x^2} + \frac{\delta_y^2}{\Delta y^2} + \frac{\delta_z^2}{\Delta z^2} \right) \omega_2$$

$$C = \frac{\delta_x}{\Delta x} (u\omega_3) + \frac{\delta_y}{\Delta y} (v\omega_3) - \frac{\delta_x}{\Delta x} (\omega_1 w) - \frac{\delta_y}{\Delta y} (\omega_2 w)$$

$$- \frac{1}{Re} \left( \frac{\delta_x^2}{\Delta x^2} + \frac{\delta_y^2}{\Delta y^2} + \frac{\delta_z^2}{\Delta z^2} \right) \omega_3$$

其中  $\Delta x, \Delta y, \Delta z$  為網格在  $x, y, z$  方向的間距， $\delta_x, \delta_y, \delta_z$  為一次中央差分運算子， $\delta_x^2, \delta_y^2, \delta_z^2$  為二次中央差分運算子。

以上的數值方法，不論在時間或空間上都可獲得二階精確度的數值解答，而數值穩定條件仍受 CFL 條件及擴散項條件控制，即

$$\left| \frac{u\Delta t}{\Delta x} \right| \leq 1, \left| \frac{v\Delta t}{\Delta y} \right| \leq 1, \left| \frac{w\Delta t}{\Delta z} \right| \leq 1 \quad (17)$$

$$\text{及 } \frac{\Delta t}{Re} \left( \frac{1}{\Delta x^2} + \frac{1}{\Delta y^2} + \frac{1}{\Delta z^2} \right) \leq \frac{1}{2} \quad (18)$$

對高雷諾數流場數值模式之數值穩定條件主要仍受(17)式控制， $\Delta t$  與網格間距同級序 (order)，對於時變問題的求解較為可行。

### 3.2 速度 Poisson 方程式之計算方法

#### (a) 速度 $u^{n+1}$

$$\left( \frac{\delta_x^2}{\Delta x^2} + \frac{\delta_y^2}{\Delta y^2} + \frac{\delta_z^2}{\Delta z^2} \right) u^{n+1} = \frac{\delta_z}{\Delta z} \omega_2^{n+1} - \frac{\delta_y}{\Delta y} \omega_3^{n+1} \quad (19)$$

$$\text{with } u^{n+1} = 0 \text{ on } x=0, M \text{ 邊界} \quad (20)$$

$$\frac{\delta_y}{\Delta y} u^{n+1} = -\omega_3^{n+1} + \frac{\delta_x}{\Delta x} v^{n+1} \text{ on } y=0, \text{N邊界} \quad (21)$$

$$\frac{\delta_z}{\Delta z} u^{n+1} = \omega_2^{n+1} + \frac{\delta_x}{\Delta x} w^{n+1} \text{ on } z=0, \text{L邊界} \quad (22)$$

在MAC交錯網格系統下（如圖一所示），以上系統可整理為

$$\nabla^2 u^{n+1} = F^* \quad (19')$$

$$\text{with } u^{n+1} = 0 \text{ on } x=0, \text{M邊界} \quad (20')$$

$$\frac{\delta_y}{\Delta y} u^{n+1} = 0 \text{ on } y=0, \text{N邊界} \quad (21')$$

$$\frac{\delta_z}{\Delta z} u^{n+1} = 0 \text{ on } z=0, \text{L邊界} \quad (22')$$

對於上述系統，我們利用快速傅利葉法(FFT)直接解出，詳細的計算方法如下：

令

$$u_{i,j+1/2,k+1/2}^{n+1} = \sum_{\ell} \sum_m \sum_n a_{\ell m n} \sin(\ell \pi x_i) \cos(m \pi y_{j+1/2}) \cos(n \pi z_{k+1/2}) \quad (23)$$

則  $u^{n+1}$  自動滿足(20')，(21')，(22')之邊界條件。

又令

$$F^* = \sum_{\ell} \sum_m \sum_n b_{\ell m n} \sin(\ell \pi x_i) \cos(m \pi y_{j+1/2}) \cos(n \pi z_{k+1/2}) \quad (24)$$

將(23)、(24)式代入(19')式中整理可得

$$a_{\ell m n} = \frac{-b_{\ell m n}}{4 \left( \frac{\sin^2 \ell \pi \Delta x}{2} + \frac{\sin^2 m \pi \Delta y}{2} + \frac{\sin^2 n \pi \Delta z}{2} \right)} \quad (25)$$

其求解程序如下：

(1)由(24)式利用快富利葉轉換求出  $b_{\ell m n}$

(2)利用(25)式計算出  $a_{\ell m n}$

(3)由(23)式利用快富利葉反轉換求出  $u^{n+1}$

對於速度的邊界條件在(21)、(22)式中，我們採用Neumann邊界條件，而不直接使用速度的Dirichlet邊界條件，這種處理方式可以不必先知道渦度之邊界值，即能解出速度場。也就是這種數值處理方法，才使得速度與渦度在求解過程中可以不需要疊代，大大的提昇數值計算的效率。

(b)速度  $v^{n+1}$

$$\left( \frac{\delta_x^2}{\Delta x^2} + \frac{\delta_y^2}{\Delta y^2} + \frac{\delta_z^2}{\Delta z^2} \right) v^{n+1} = \frac{\delta_x}{\Delta x} \omega_3^{n+1} - \frac{\delta_z}{\Delta z} \omega_1^{n+1} \quad (26)$$

$$\text{with } \frac{\delta_x}{\Delta x} v^{n+1} = \omega_3^{n+1} + \frac{\delta_y}{\Delta y} u^{n+1} \text{ on } x=0, \text{M邊界} \quad (27)$$

$$v^{n+1} = 0 \text{ on } y=0, \text{N邊界} \quad (28)$$

$$\frac{\delta_z}{\Delta z} v^{n+1} = -\omega_1^{n+1} + \frac{\delta_y}{\Delta y} w^{n+1} \text{ on } z=0, \text{L邊界} \quad (29)$$

整個系統與  $u^{n+1}$  相似，故數值計算方法與解  $u^{n+1}$  相同，不再贅述。

(c)速度  $w^{n+1}$  之計算方法

$w^{n+1}$  可由  $w$  的 Poisson 方程式中直接解出，但也可由連續方程式(1)式中計算出來，本文由(1)式中解出，其計算方法如下：

由(1)式

$$\frac{\delta_z}{\Delta z} w^{n+1} = -\left( \frac{\delta_x}{\Delta x} u^{n+1} + \frac{\delta_y}{\Delta y} v^{n+1} \right) \quad (30)$$

對  $z$  方向微分一次可得

$$\frac{\delta_z^2}{\Delta z^2} w^{n+1} = -\frac{\delta_z}{\Delta z} \left( \frac{\delta_x}{\Delta x} u^{n+1} + \frac{\delta_y}{\Delta y} v^{n+1} \right) \quad (31)$$

$$\text{with } w^{n+1} = 0 \text{ on } z=0, \text{L} \quad (32)$$

利用(31)、(32)式直接計算出  $w^{n+1}$ ，由於僅為三對角線代數系統故很容易求解。

### 3.3 數值計算程序

1.給定流場初始及邊界條件

2.由(14)、(15)、(16)式中計算所有內點的  $\omega_1^{n+1}, \omega_2^{n+1}, \omega_3^{n+1}$ 。

3.由(19)、(20)、(21)、(22)式中利用FFT解出  $u^{n+1}$ 。

4.由(26)、(27)、(28)、(29)式中利用FFT解出  $v^{n+1}$ 。

5.由(31)、(32)式中解出  $w^{n+1}$ 。

6.設定  $u^{n+1}, v^{n+1}, w^{n+1}$  及  $\omega_1^{n+1}, \omega_2^{n+1}, \omega_3^{n+1}$  之邊界值。

7.重覆2~6直到所求時間之流場解。

## 四、計算結果與討論

### 4.1 數值模式之驗證

利用速度一渦度法來求解三維流動問題，模式建立成功後，我們以三維穴流問題進行驗證前人的工作。在一長寬高為  $1:3:1$  的長方形渠槽中，上板以  $u=1$  的速度拖動，流場示意圖如圖二所示。數值計算以  $Re=1500$  為模擬對象，採用  $48 \times 144 \times 48$  的網格系統， $\Delta t=0.01$ 。數值計算所採用的網格為  $u, v, w$ ，及  $\omega_1, \omega_2, \omega_3$  交錯配置的網格系統，如圖一所示。這種變數交互配置的網格系統，在邊界條件上的處理有很大的優點，即速度與渦度在求解過程不需要疊代程序。圖三為數值計算結果之流場解答，經與蔣(1996)之結果比較，如圖四，證實數值模式確實無誤。

### 4.2 數值計算結果

本文以三維穴流及三維後向階梯流流場進行數值計算工作，數值計算結果分別討論如下：

#### (一)三維方型穴流

我們以  $1:1:1$  的三維方型穴流問題，進行流場模擬，計算結果如下：

1.  $Re=1000, 48 \times 48 \times 48$  網格，流場穩定解如圖五所示。(a)圖為三維切面流線圖，在靠近邊界及中心流線較密，速度較快，中間帶之流線較稀疏，流速較慢；(b)圖為三維流線圖，其水流繞中心以逆時鐘方向轉動，流況非常穩定；(c)圖為向量圖，可看出在頂部之水流作用力量相當大，中央之水流作用較小；(d)圖為(a)圖為之二維流線，左下角之迴流區比右下角之迴流區大，兩迴流內之轉動方向與主要迴流區轉動相反，為順時鐘；(e)圖為(d)圖左下角迴流

區放大圖，在中心及邊界之迴流較強，流線由下向上以順時鐘旋轉；(f)圖為(d)圖右下角迴流區放大圖，水流流動方向為順時鐘，流況正在發展中；(g)圖為(d)圖右上角迴流區放大圖，流線上升至頂部時，遇到強大的水流，使流線作接近90度的轉彎，在頂部速度異常大。

2.  $Re=2000$ ， $72 \times 72 \times 72$  網格，流場已為暫態(Transient)，不再具有穩態解。其流場解答繪於圖六中。可以看出較  $Re=1000$  之流況更強烈；其中右下角之迴流區變大，流線改由上向下以順時鐘旋轉，右下角及左下角迴流區間有一狹長之流線分離區。整個流況非常穩定，數值計算結果相當可靠。

## (二)三維後向梯流場

根據Arnaly *et al.* (1983)之實驗，長150mm，寬180mm，高10.1mm之渠道中，入流渠道高5.2mm，階梯高4.9mm，如圖七所示。由於具對稱關係，數值計算取只一半寬，渠長則取30倍階梯高，來進行數值模擬。入流條件係由充分發展之矩形斷面流之解析解代入模式中。在層流範圍上述的入流條件與實驗相當一致，故吾人採用上述的入流條件進行了  $Re=100$ ， $200$ ， $300$ ， $397$ ， $500$ ， $600$ ， $648$ ， $800$  等案例之計算，一律採用  $128 \times 64 \times 32$  的網格系統，計算結果如圖八、九所示，圖八為雷諾數  $100$ ， $200$ ， $300$ ， $397$ ，圖九則為雷諾數  $500$ ， $600$ ， $648$ ， $800$  等中央對稱面速度  $u$  之等值線圖，左下角落有一迴流區。我們將渠道中央對稱面 ( $y=0$ 處) 階梯後迴流泡之再接觸長度  $X_r$  與雷諾數  $Re$  之關係繪於圖十，由圖中可以看出數值計算結果與實驗值相當一致，這是一般二維模式無法達到的。對於  $Re=800$  的案例，我們再將其流場解答繪於圖十一。由(a)圖中可看出，除了在階梯後方出現一個大迴流區外，在上邊界  $X=15$  處，亦產生一迴流區，其流線相當密集，流況非常激烈；(b)圖為三維流線圖，受到階梯之影響，後方之迴流區相當大，流場解答非常不錯。經過初步的數值模擬結果顯示，本文所提出的速度—渦度法確實可以應用於三維不可壓縮流之求解上。

## 五、結論

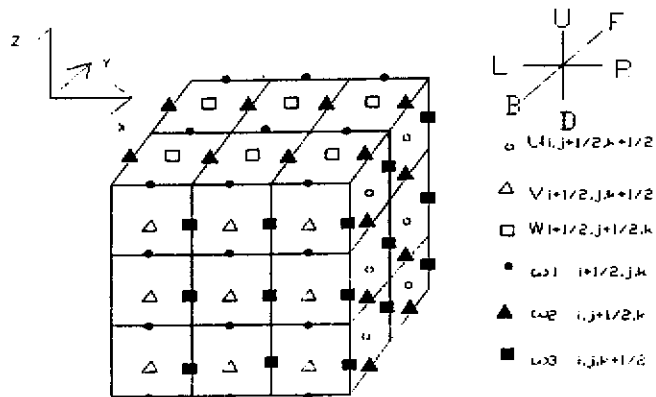
1. 本文以速度—渦度列式法來求解三維不可壓縮流動問題，經三維穴流及三維後向階梯流兩案例與前人研究之數值及實驗結果的比較後，證實數值模式相當成功。數值模式採用交錯網格配置，使得在二階精確度下，渦度與速度在求解過程不需要疊代程序，大大地提升了數值計算效率。
2. 在後向階梯流的案例中，其出流條件採用線性對流條件，即在出口附近流體係以平均速度向下游傳遞，確實是一種相當不錯的處理方式。
3. 以速度—渦度列式法求解三維流場，需解六條方程式，較原來 Navier-Stokes 方程式多出二條，但連續方程式可自動滿足，因此仍值得採用。
4. 本文所有計算都在個人電腦上執行，而不必使用大型主機或工作站。將來可朝平行計算發展，改善數值計算速度。

## 誌謝

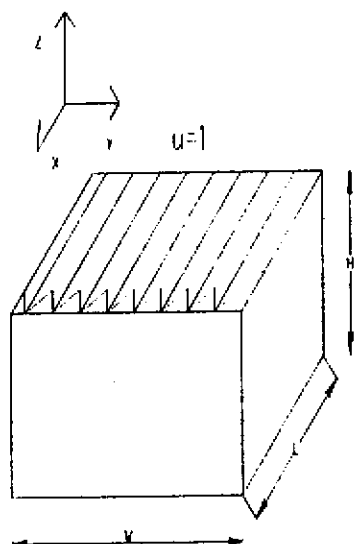
本研究成承蒙行政院國家科學委員會之經費贊助，(計畫編號：NSC88-2611-E-002-030) 謹致謝意。

## 參考文獻

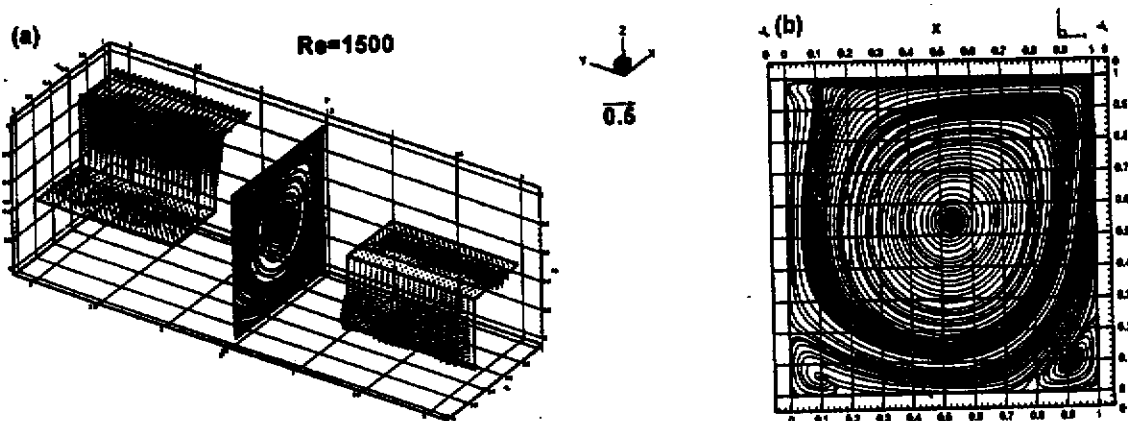
1. Arnaly, B., Durst, F. F., Pereira, J. C. F. and Schonung, B., 1983, "Experiment and theoretical investigation of backward-facing step flow," *J. Fluid Mech.*, 127, pp. 473.
2. Babu, V. and Korpela, S. A., 1994, "Numerical solutions of the incompressible, three-dimensional Navier-Stokes equations," *Computer Fluids*, Vol.23, No. 5, pp.675-691.
3. Burggraf, O. R., 1966, "Analytical and numerical studies of the structure of steady separated flows," *J. Fluid Mech.*, 24(1), pp.113-151.
4. Chiang, T. P., Hwang, R. R. and Sheu, W. H. 1996, "Some physical insights inside a Lid-driven Rectangular Cavity," 第十三屆全國機械工程研討會論文集，pp. 99-104.
5. Fusegi, T. and Farouk, B., 1986, "Predictions of Fluid and Heat Transfer Programs by the Vorticity-Velocity Formulation of the Navier-Stokes Equation and a Multigrid Method," *J. Comput. phys.*, 48, pp.387-411.
6. Ghia, U., Ghia, K. N. and Shin, C., T., 1982, "High-Re Solutions for Incompress Flow Using the Navier-Stokes Equations and a Multigrid Method," *J. Comput. phys.*, 48, pp.387-411.
7. Giannattasio, P., and Napolitano, M., 1996, "Optimal Vorticity Conditions for the Node-Centerer Finite-Difference Discretization of the Second-Order Vorticity-Velocity Equations," *J. Comput. phys.*, 127, pp.208-217.
8. Pan, F., and Acrivos, A., 1967, "Steady flows in rectangular cavities," *J. Fluid Mech.*, Vol.28, PP643-655.
9. 廖清標、許正元、賴仲愷，1995，“利用速度—渦度列式法來求解不可壓縮流”，第四屆全國計算流體力學研討會論文集，pp.73-81。
10. 劉英宏、楊德良，1998，“利用速度渦度法解析三維黏性不可壓縮流場”，第二十二屆全國力學會議論文集第二冊，pp.339-345。



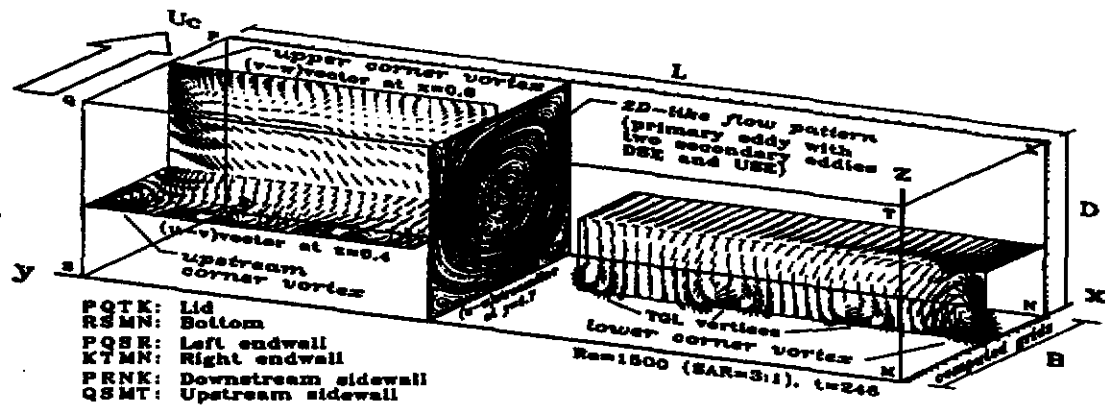
圖一 三維流場之網格配置圖



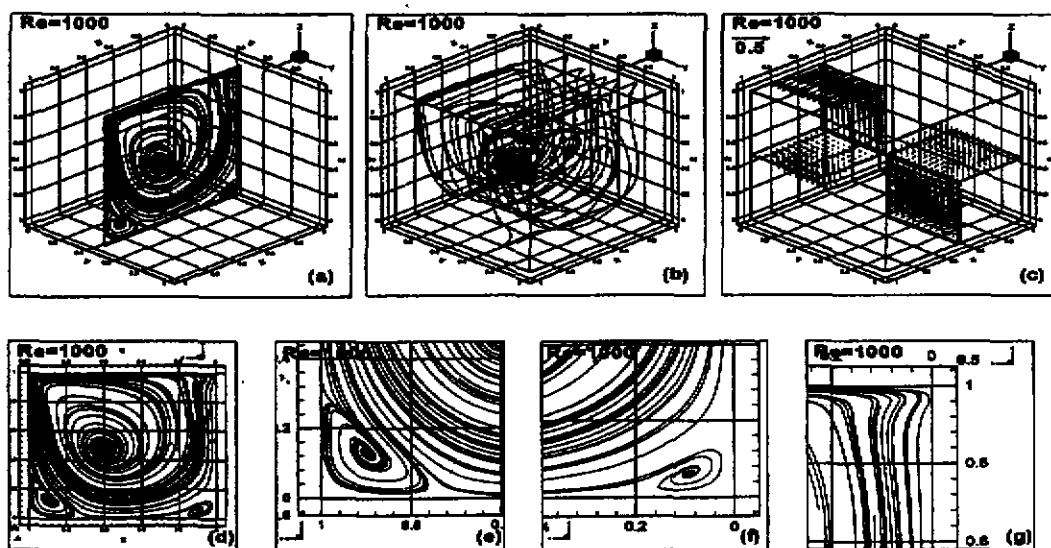
圖二 三維穴流流場示意圖



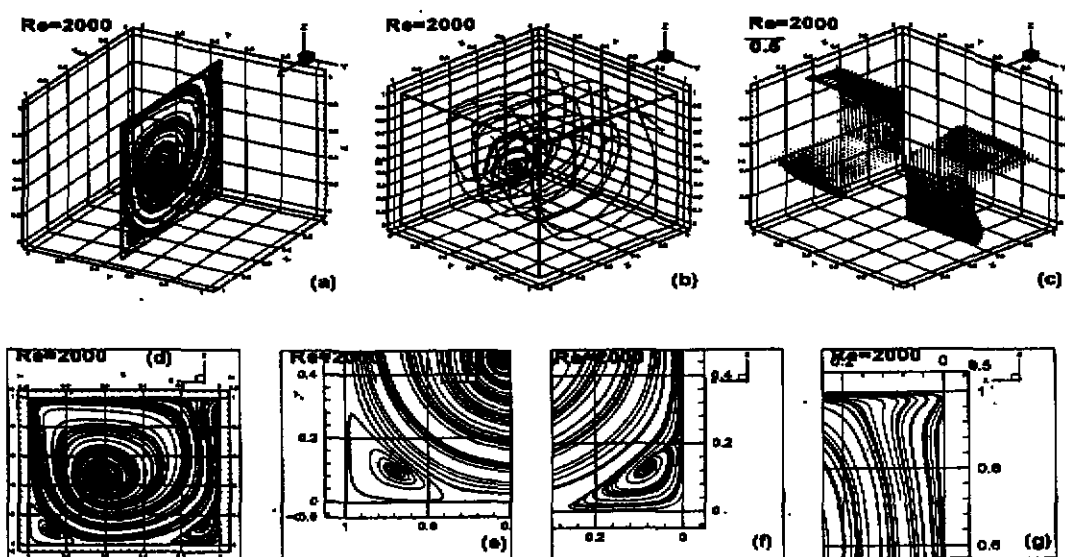
圖三 三維穴流  $Re=1500$  之數值模擬圖



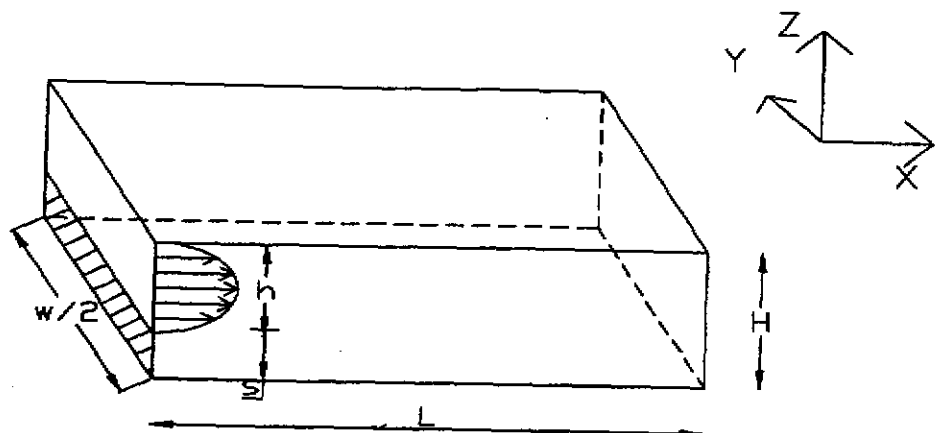
圖四 三维穴流 $Re=1500$ 之流場 (蔣, 1996)



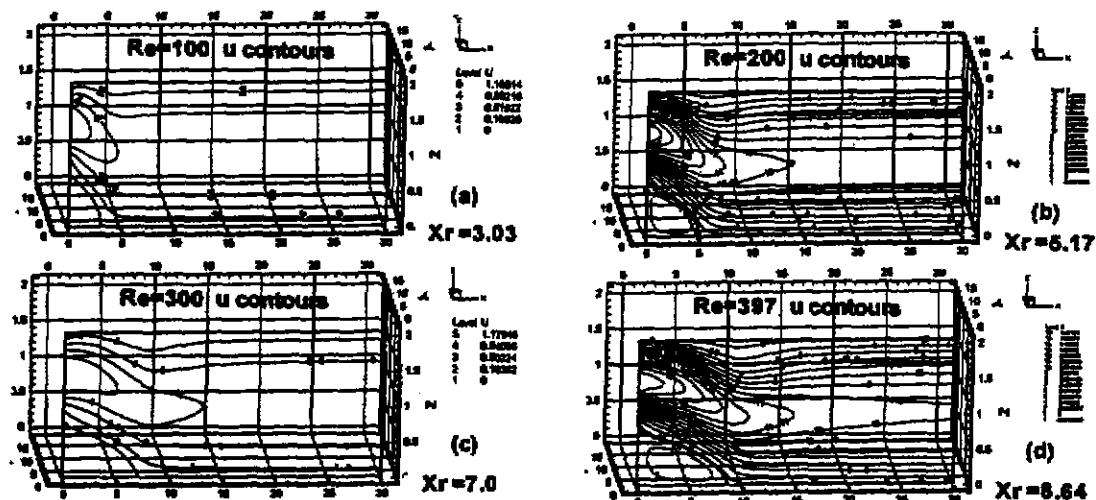
圖五 三维穴流 $Re=1000$ 之數值模擬圖



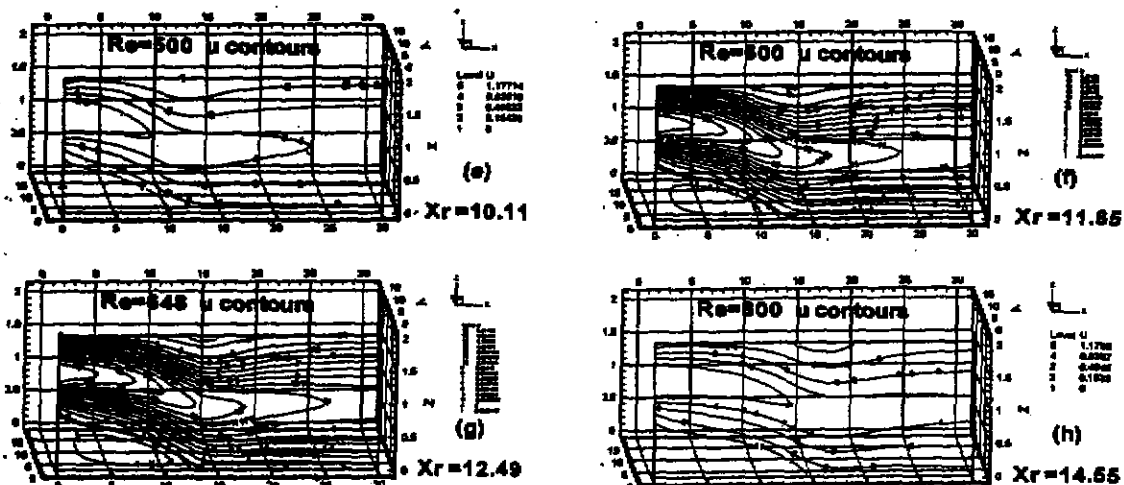
圖六 三维穴流 $Re=2000$ 之數值模擬圖



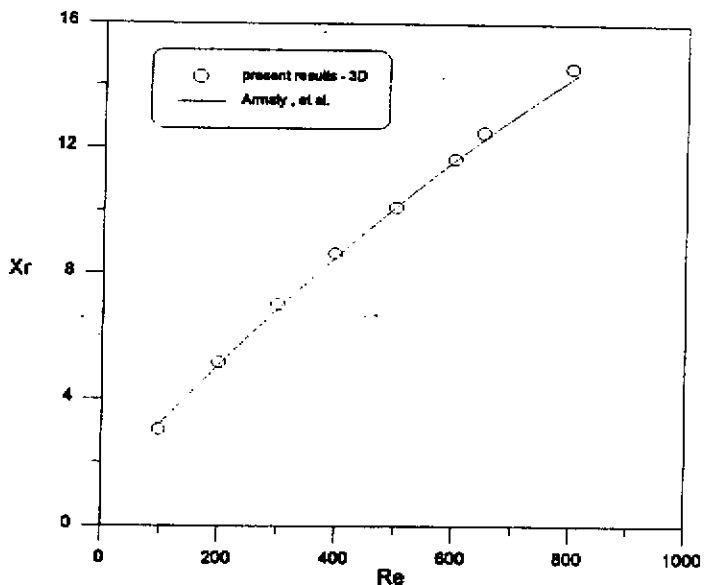
圖七 三維後向階梯流流場示意圖



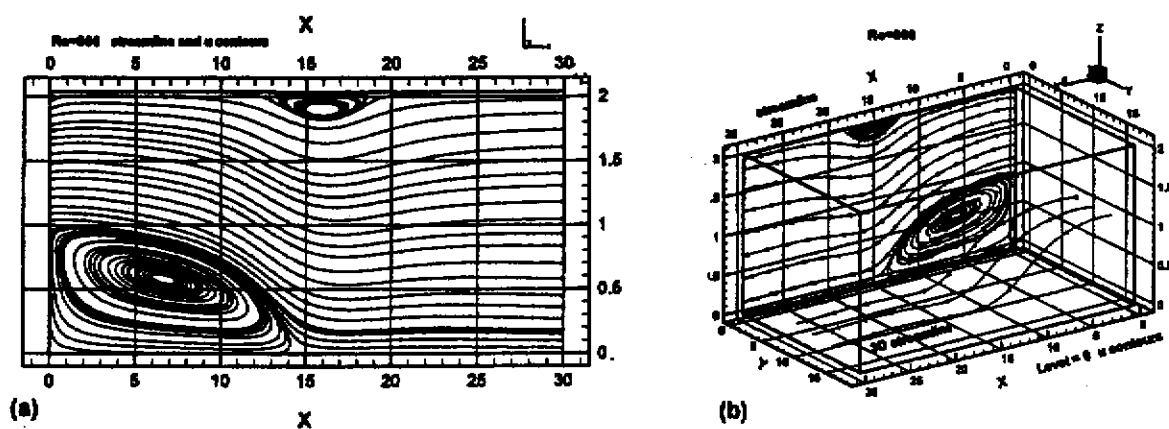
圖八 三維後向階梯流  $Re=100, 200, 300, 397$  對稱面之流線圖



圖九 三維後向階梯流  $Re=500, 600, 648, 800$  對稱面之流線圖



圖十 三維後向階梯流再接觸長度 $X_r$ 與RE數關係實驗與數值模式比較圖



圖十一 三維後向階梯流 $Re=800$ 之流線圖

B6. Liao, C.B., Wu, M.F., Lu, T.C., and Young, D.L., 1999, "Numerical Simulation for the Three-dimensional Backward Facing Step Flow", The Proceedings of the 23<sup>rd</sup> National Conference on Mechanics, Hsin-chu, Vol. 1, pp.224-231(in Chinese).

# 三維後向階梯流之數值模擬

廖清輝<sup>1</sup> 袁泰成<sup>2</sup> 吳銘峰<sup>1</sup> 楊達貞<sup>3</sup>

1.逢甲大學土木及水利工程研究所

2.逢甲大學土木工程系

3.台灣大學土木系教授兼水工試驗所

## 摘要

本研究發展一準確、有效率之數值計算方法，求解具開放邊界之三維不可壓縮性流動問題，以後向階梯流場為對象，進行初步數值計算工作。將Navier-Stokes方程式以速度—渦度法來列式，並以有限差分法求解。數值模式以顯示Adams-Basforth法，來求解Helmholtz渦度傳輸方程式；對速度之Poisson方程式則利用快速傅利葉轉換法直接求解。配合交錯網格系統，在求解過程不需要渦度的邊界條件，且速度和渦度場在求解過程不用疊代，大大提高計算效率，數值解對時間及空間皆為二階精確度。數值模擬各種不同之Reynolds數之流場穩態解，經與他人實驗結果比較相當成功。本數值方法，當可應用於其他三維不可壓縮流場的數值模擬上。

關鍵詞：速度—渦度法，三維流，後向階梯流，Helmholtz方程式，Poisson方程式。

## 一、前言

內流場因斷面幾何形狀之突然改變，常會使流場形成分流(Flow separation)現象，此種流場型態亦普遍存在於工程上，如研究單雙後向階梯流場渠道斷面之突然擴大及渠流越流過一階梯之流動問題，隨入流及渠流越過障礙比例不同，流場亦會有不同變化。因此有眾多學者投入相關之實驗、理論及數模分析之研究。

欲了解分流區之流場特性，Abbott and kiine [1] 以實驗探討單後向階梯及雙後向階梯次音速流場，其研究結果發現紊流分流區有三流況(Flow regimes)存在，包括三維流況、二維流況及時變性之尾流區。Goldstein等人[2]以實驗研究單雙後向階梯流場之層流分離，再附著與過渡流(Transition flow)，其結果得到層流之再接觸長度和Reynolds數成正比。

Armaly[3]等人以實驗及數值方法探討後向階梯流場，提出流速分佈及再接觸長度資料，其流場Reynolds範圍在70至8000之間，涵蓋層流、過渡流及紊流流況，同時亦進行層流流場之數值計算工作。

至於後向階梯流場特點，為入流渠流流向一類似階梯之突擴區域，使原在入流段發展之流場受邊界變化之影響，促使流場出現變化，且隨入流之長寬不同及速度不同流場會有不同變化。本研究將以速度—渦度法來求解三維的後向階梯流場，並以Armaly等人之實驗資料來驗證數值模式之可靠性。速度—渦度法是利用渦度傳輸擴散方程式，及速度的Poisson方程式來求解流場，其主要困難在於渦度的邊界條件之處理及速度與渦度間互相關聯，必需疊代求解。利用本方法來求解流場如Fusegi and Farouk [4]，Giannattasio and Napolitano [5]，劉與楊等[6]。本文將廖等人[7]之二維模式推廣至三維流場，利用有限差分交錯網格(staggered grid system)，不需要渦度的邊界條件，且速度與渦度在求解過程不須疊代程序，數值計算結果顯示本研究之數值模式相當成功。本數值計算方法，當可應用於其他具開放邊界流動問題之數值模擬上。

## 二、控制方程式

### 2.1 不可壓縮Navier-Stokes方程式

$$\nabla \cdot \vec{u} = 0 \quad (1)$$

$$\frac{\partial \vec{u}}{\partial t} + \vec{u} \cdot \nabla \vec{u} = -\nabla p + \frac{1}{Re} \nabla^2 \vec{u} \quad (2)$$

式中  $\vec{u} = u\vec{i} + v\vec{j} + w\vec{k}$  為流體速度， $p$  為流體壓力， $Re$  為 Reynolds number， $Re = VL/\nu$ ， $V$  為特性速度， $L$  為特性長度， $\nu$  為流體運動粘滯性係數。

### 2.2 涡度 $\vec{\omega}$ 方程式

$$\vec{\omega} = \nabla \times \vec{u} \quad (3)$$

式中

$$\vec{\omega} = \omega_1 \vec{i} + \omega_2 \vec{j} + \omega_3 \vec{k}$$

而各分量分別為

$$\omega_1 = \frac{\partial v}{\partial y} - \frac{\partial u}{\partial z} \quad (4)$$

$$\omega_2 = \frac{\partial u}{\partial z} - \frac{\partial w}{\partial x} \quad (5)$$

$$\omega_3 = \frac{\partial w}{\partial x} - \frac{\partial v}{\partial y} \quad (6)$$

### 2.3 涡度傳輸方程式

對(2)式取旋度(curl)，可得

$$\frac{\partial \vec{\omega}}{\partial t} - \nabla \times (\vec{u} \times \vec{\omega}) = \frac{1}{Re} \nabla^2 \vec{\omega} \quad (7)$$

(7)式可進一步寫成

$$\frac{\partial \vec{\omega}}{\partial t} + \vec{u} \cdot \nabla \vec{\omega} = \vec{\omega} \cdot \nabla \vec{u} + \frac{1}{Re} \nabla^2 \vec{\omega} \quad (8)$$

我們可利用(7)或(8)式來求解渦度。(8)式一般稱為Helmholtz渦度傳輸方程式。

### 2.4 速度的Poisson方程式

由(4)-(6)式及(1)式，吾人可推導出速度必須滿足下列方程式

$$\nabla^2 u = \frac{\partial \omega_2}{\partial z} - \frac{\partial \omega_3}{\partial y} \quad (9)$$

$$\nabla^2 v = \frac{\partial \omega_3}{\partial x} - \frac{\partial \omega_1}{\partial z} \quad (10)$$

$$\nabla^2 w = \frac{\partial \omega_1}{\partial y} - \frac{\partial \omega_2}{\partial x} \quad (11)$$

所謂速度—渦度就是利用(7)或(8)式配合(9)-(11)式來求解流場，而不由原來的 Navier-Stokes方程式來求解。由於速度及渦

度都是向量，在三維流場中共有6個變數待解，較原來問題4個變數要多解二條方程式，故一般很少使用這種方法來求解三維流動問題，但本文嘗試此方法來求解，在數值模式中為一大挑戰。

## 三、數值計算方法

### 3.1 涡度方程式的計算方法

利用顯式二階Adams-Basforth法來離散(7)式，可得

$$\frac{\omega_1^{n+1} - \omega_1^n}{\Delta t} + 1.5A^n - 0.5A^{n-1} = 0 \quad (12)$$

$$\frac{\omega_2^{n+1} - \omega_2^n}{\Delta t} + 1.5B^n - 0.5B^{n-1} = 0 \quad (13)$$

$$\frac{\omega_3^{n+1} - \omega_3^n}{\Delta t} + 1.5C^n - 0.5C^{n-1} = 0 \quad (14)$$

式中

$$A = \frac{\delta_y}{\Delta y}(v\omega_1) + \frac{\delta_z}{\Delta z}(w\omega_1) - \frac{\delta_y}{\Delta y}(\omega_2 u) - \frac{\delta_z}{\Delta z}(\omega_3 u) \\ - \frac{1}{Re} \left( \frac{\delta_x^2}{\Delta x^2} + \frac{\delta_y^2}{\Delta y^2} + \frac{\delta_z^2}{\Delta z^2} \right) \omega_1$$

$$B = \frac{\delta_x}{\Delta x}(u\omega_2) + \frac{\delta_z}{\Delta z}(w\omega_2) - \frac{\delta_x}{\Delta x}(\omega_1 v) - \frac{\delta_z}{\Delta z}(\omega_3 v) \\ - \frac{1}{Re} \left( \frac{\delta_x^2}{\Delta x^2} + \frac{\delta_y^2}{\Delta y^2} + \frac{\delta_z^2}{\Delta z^2} \right) \omega_2$$

$$C = \frac{\delta_x}{\Delta x}(u\omega_3) + \frac{\delta_y}{\Delta y}(v\omega_3) - \frac{\delta_x}{\Delta x}(\omega_1 w) - \frac{\delta_y}{\Delta y}(\omega_2 w) \\ - \frac{1}{Re} \left( \frac{\delta_x^2}{\Delta x^2} + \frac{\delta_y^2}{\Delta y^2} + \frac{\delta_z^2}{\Delta z^2} \right) \omega_3$$

其中  $\Delta x, \Delta y, \Delta z$  為網格在  $x, y, z$  方向的間距， $\delta_x, \delta_y, \delta_z$  為一次中央差分運算子， $\delta_x^2, \delta_y^2, \delta_z^2$  為二次中央差分運算子。

以上的數值方法，不論在時間或空間上都可獲得二階精確度的數值解答，而數值穩定條件仍受CFL條件及擴散項條件控制，即

$$\left| \frac{u\Delta t}{\Delta x} \right| \leq 1, \left| \frac{v\Delta t}{\Delta y} \right| \leq 1, \left| \frac{w\Delta t}{\Delta z} \right| \leq 1 \quad (15)$$

及

$$\frac{\Delta t}{\text{Re}} \left( \frac{1}{\Delta x^2} + \frac{1}{\Delta y^2} + \frac{1}{\Delta z^2} \right) \leq \frac{1}{2} \quad (16)$$

對中高 Reynolds 數流場， $\Delta t$  與網格間距同級序（order），對於時變問題的求解較為可行。

### 3.2 速度Poisson方程式之計算方法

#### 1. 速度 $u^{n+1}$ 之計算方法

由 (9) 式可得

$$\left( \frac{\delta_x^2}{\Delta x^2} + \frac{\delta_y^2}{\Delta y^2} + \frac{\delta_z^2}{\Delta z^2} \right) u^{n+1} = \frac{\delta_z}{\Delta z} \omega_2^{n+1} - \frac{\delta_y}{\Delta y} \omega_3^{n+1} \quad (17)$$

$$u^{n+1} = 0 \quad \text{on } x=0, M \text{邊界} \quad (18)$$

$$\frac{\delta_y}{\Delta y} u^{n+1} = -\omega_3^{n+1} + \frac{\delta_x}{\Delta x} v^{n+1} \quad \text{on } y=0, N \text{邊界} \quad (19)$$

$$\frac{\delta_z}{\Delta z} u^{n+1} = \omega_2^{n+1} + \frac{\delta_x}{\Delta x} w^{n+1} \quad \text{on } z=0, L \text{邊界} \quad (20)$$

在MAC交錯網格系統下（如圖一所示），以上系統可整理為

$$\nabla^2 u^{n+1} = F^* \quad (17-1)$$

$$u^{n+1} = 0 \quad \text{on } x=0, M \text{邊界} \quad (18-1)$$

$$\frac{\delta_y}{\Delta y} u^{n+1} = 0 \quad \text{on } y=0, N \text{邊界} \quad (19-1)$$

$$\frac{\delta_z}{\Delta z} u^{n+1} = 0 \quad \text{on } z=0, L \text{邊界} \quad (20-1)$$

我們利用快速傅利葉法(FFT)直接解出，詳細的計算方法在此從略。

#### 2. $v^{n+1}$ 之計算方法

由 (10) 式可得

$$\left( \frac{\delta_x^2}{\Delta x^2} + \frac{\delta_y^2}{\Delta y^2} + \frac{\delta_z^2}{\Delta z^2} \right) v^{n+1} = \frac{\delta_x}{\Delta x} \omega_3^{n+1} - \frac{\delta_z}{\Delta z} \omega_1^{n+1} \quad (21)$$

$$\frac{\delta_x}{\Delta x} v^{n+1} = \omega_3^{n+1} + \frac{\delta_y}{\Delta y} u^{n+1} \quad \text{on } x=0, M \text{邊界} \quad (22)$$

$$v^{n+1} = 0 \quad \text{on } y=0, N \text{邊界} \quad (23)$$

$$\frac{\delta_z}{\Delta z} v^{n+1} = -\omega_1^{n+1} + \frac{\delta_y}{\Delta y} w^{n+1} \quad \text{on } z=0, L \text{邊界} \quad (24)$$

整個系統與  $u^{n+1}$  相似，故數值計算方法與解  $u^{n+1}$  相同。

### 3.3 $w^{n+1}$ 之計算方法

$w^{n+1}$  可由  $w$  的 Poisson 方程式中直接解出，但也可由連續方程式(1)式中計算出來，本文由(1)式中解出，其計算方法如下：

由(1)式

$$\frac{\delta_z}{\Delta z} w^{n+1} = -\left( \frac{\delta_x}{\Delta x} u^{n+1} + \frac{\delta_y}{\Delta y} v^{n+1} \right) \quad (25)$$

對  $z$  方向微分一次可得

$$\frac{\delta_z^2}{\Delta z^2} w^{n+1} = -\frac{\delta_z}{\Delta z} \left( \frac{\delta_x}{\Delta x} u^{n+1} + \frac{\delta_y}{\Delta y} v^{n+1} \right) \quad (26)$$

$$w^{n+1} = 0 \quad \text{on } z=0, L \text{邊界} \quad (27)$$

利用(26)、(27)式直接計算出  $w^{n+1}$ ，由於僅為三對角線代數系統故很容易求解。

### 3.4 邊界條件之處理

後向階梯流場如圖二所示，其邊界條件如下：

(1) 入流邊界條件 ( $x=0$ )

矩形斷面充份發展層流，以解析解給定。

(2) 出流邊界條件 ( $x=L$ )

$$\frac{\partial u}{\partial x} + V \frac{\partial u}{\partial x} = 0 \quad , V \text{為平均入流速度。}$$

(3) 壁面不可滑動條件 ( $z=0, z=H, y=\frac{D}{2}$ )

$$u = v = w = 0$$

(4) 對稱面對稱條件 ( $y=0$ )

$$v=0 \quad , \quad \frac{\partial u}{\partial y} = \frac{\partial w}{\partial y} = 0$$

在數值計算中我們仍使用速度之物理邊界條件，至於渦度之邊界值可由(4)、(5)、(6)式中求出。由於採用交錯網格系統，配合本文提出的數值方法，求解過程不必使用渦度邊界值，當速度解出後再計算出渦度之邊界值即可，這樣又可避免速度與渦度間的疊代程序。

### 3.5 數值計算程序

1. 細定流場初始及邊界條件

2. 由(12)、(13)、(14)式中計算所有內點  $\omega_1^{n+1}, \omega_2^{n+1}, \omega_3^{n+1}$ 。

3. 由(17)、(18)、(19)、(20)式中解  $u^{n+1}$ 。

4. 由(21)、(22)、(23)、(24)式中解出

$$v^{n+1}.$$

5. 由(26)、(27)式中解  $w^{n+1}$ 。

6. 設定  $u^{n+1}, v^{n+1}, w^{n+1}$  及  $\omega_1^{n+1}, \omega_2^{n+1}, \omega_3^{n+1}$  之邊界值。

7. 重覆2~6直到所求時間之流場解。

#### 四、計算結果與討論

##### 4.1 數值模式之驗證

本文以後向階梯流場為對象，流場示意圖如圖二所示進行數值模擬計算。後向階梯流場為測試數值方法是否準確的一個很好案例，因為分流區再附著點之長度  $X_r$  與 Reynolds 數有關，準確的數值計算方法才能正確的預測  $X_r$  長度。根據 Armaly et al. (1983) 之實驗，長 150mm，寬 180mm，高 10.1mm 之渠道中，入流渠道高 5.2mm，階梯高 4.9mm，如圖三所示，由於具對稱關係，數值計算取只一半寬，渠長則取 30 倍階梯高，來進行數值模擬。入流條件係由充分發展之矩形斷面流之解析解代入模式中，在層流範圍，上述的入流條件與實驗相當一致，故吾人採用上述的入流條件，進行了  $Re=100, 200, 300, 397, 500, 600, 648, 800$  等案例之計算，採用  $128 \times 64 \times 32$  的網格系統，渠道中央對稱面 ( $y=0$ 處) 階梯後之再接觸長度  $X_r$  與雷諾數之關係繪於圖三，由圖中可看出數值計算結果與實驗值相當一致。

##### 4.2 數值計算結果

1.  $Re=200, 128 \times 32 \times 64$  網格， $t = 45.9835$

圖四為取中央切面  $u$  之二維流線圖，圖中可明顯看出入流口之速度值最大往上下兩邊界呈遞減，在左下角流線因受入流口之突擴，而使流線往下沿壁面發展形成逆向壓力梯度和慣性速度相反，此時壓力梯度和粘滯力共同消抵慣性速度，使邊界層厚度迅速加厚並在左下角形成迴流現象。而在迴流區後面者之流線平直且無分離情形，顯示該區粘滯力大於慣性速度，所以流場呈現規則。圖五為取第一切面  $u$  之二維等值線，其流況情形如流線圖一般，可明顯看出分流區範圍及階梯後迴流泡之再接觸長度  $X_r=5.17$ 。

2.  $Re=397, 128 \times 32 \times 64$  網格， $t = 99.4098$

圖六為流場達穩態時  $u$  之二維流線及等值線圖，圖中可清楚看出左下角迴流區範圍往渠道下游擴大，階梯後之再接觸長度  $X_r=8.64$ 。而且在上壁之等值線圖中有一微小區域其值為 0.00637，若 Reynolds 再加大，上壁即可出現另一迴流區。另從圖七之三維流線圖確可看到上壁處迴流區之雛形漸形成，此即受上壁邊界影響所致。在左下角之迴流區由中央對稱面往左邊界壁逐漸縮小，亦是受邊界影響速度梯度所致。

3.  $Re=600, 128 \times 32 \times 64$  網格， $t = 223.143$

此時再將  $Re$  加大至 600，圖八為流場達穩態時之二維流線及等值線圖，圖中左下角迴流區範圍更擴大， $X_r=11.65$  亦往下游渠道成長移動，而上壁邊界處之迴流區已清楚可見，其和上邊界接觸之範圍為  $X_r=14.18, X_r=11.64$ 。再由圖九三維流線圖亦可看出上下兩處迴流區產生。

4.  $Re=800, 128 \times 32 \times 64$  網格， $t = 258.498$

最後模擬  $Re=800$  之流場，圖十為穩態時流場解答，圖中可清楚看出分流之範圍更加擴大及渠道中水流流動情況，階梯後之迴流區和上壁迴流區流動情況，最大流速發生在中央偏上。 $X_r$  已延伸至 14.55，上分流區也略往下游移動並稍為擴大， $X_r=19.14, X_r=14.46$ 。圖十一為三維向量圖及取切面  $u$  之等值線圖，圖中可看出邊壁對流場之影響並隨往下游區產生變化，再從點選之流線中可看出隨渠道發展而由一個迴流增加為二個，且在靠邊壁之角落有一角迴流 (corner vortex)，此即受二次迴流 (secondary flow) 所致，這亦將是更高  $Re$  時會產生不穩定原因。

#### 五、結論

1. 本文以速度 - 渦度列式法來求解三維不可壓縮流動問題，經三維後向階梯流案例與前人研究之實驗結果比較後，證實數值模式相當成功。數值模式採用交錯網格配置，使得在二階精確度下，渦度與速度在求解過程不需要疊代程序，大大地提昇數值計算效率。
2. 在後向階梯流的案例中，其出流條件採用線性對流條件，即在出口附近流體係以平均速度向下游傳遞，確實是一種相當不錯的處理方式。

3. 本研究以渦度-速度列式法求解三維流場，需解六條方程式，較原來Navier-Stokes方程式多出二條，但連續方程式可自動滿足，且渦度與速度不必疊代，因此仍值得採用。
4. 相關研究發現，本流場之渠道高度比不同，對流場影響甚大，本文侷限於固定渠道高度情況下作初步研究，後續將對不同渠道高度比作更深入探討。

### 誌謝

本研究承蒙行政院國家科學委員會之經費贊助，（計畫編號：NSC88-2611-E-002-030）謹致謝意。

### 參考文獻

1. Abbott, D. E. and Kline, S. J. "Experimental Investigation of Subsonic Turbulent Flow over single and Double Backward Facing Steps", Trans. ASME, D : J. basic Engng 84 , PP317-325, 1962.
2. Filetti, W. G. and Kays, W. W. "Fleat Trallsfer in Separtes, Reattached, and Redevelopment Regions Behind a Double Step at Entrance to a Flat Duct", Trans. Asme, C : J. Heat Transfer 89 PP163-325, 1967.
3. Armaly, B. F. Durst, F., Pereira J. C. F. and Schonung, B. 1983,"Experiment and theoretical investigation of backward-facing step flow", J. Fluid Mech., 127, pp. 473.
4. Fusegi, T. and Farouk, B., 1986,"Pedictions of Fluid and Heat Transfer Programs by the Vorticity-Velocity Formulation of the Navier-Stokes Equations.", J. Comput, phys., 127, pp.208-217.
5. Giannattasio, P., and Napolitano, M., 1996,"Optimal Vorticity Conditions for the Node-Centerer Finite-Difference Discretization of the Second-Order Vorticity-Velocity Equations.", J. Comput, phys., 127, pp.208-217.
6. 劉英宏、楊德良，1998 “利用速度渦度法解析三維黏性不可壓縮流場”，第二屆全國力學會議論文集第二冊，pp.339-345。
7. 廖清標、許正元、顧仲愷，1995 “利用速度-渦度列式法來求解不可壓縮流”，第四屆全國計算流體力學研討會論文集，pp.73-81。

## NUMERICAL SIMULATION FOR THE THREE-DIMENSIONAL BACKWARD-FACING STEP FLOW

Ching-Biao Liao M. F. Wu

The Graduate Institute of Civil and Hydraulic Engineering Feng Chia University

T. C. Lu

Department of Civil Engineering, Chen Kuo Jr.

College of Technology Commerce

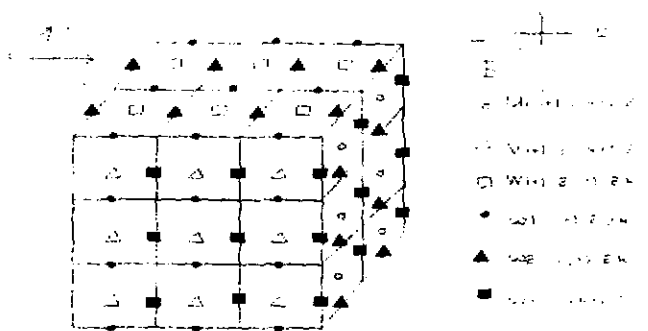
Der-Liang Young

Department of Civil Engineering and Hydrotech Laboratory, National Taiwan University

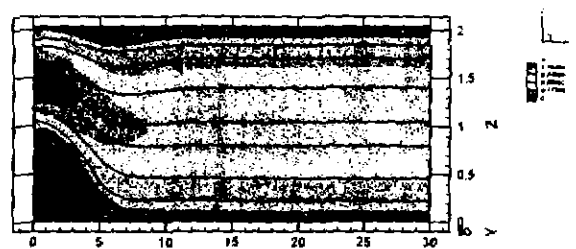
### ABSTRACT

We presented an efficient, accurate numerical scheme to solve the incompressible flow with open boundary problem. The three-dimensional backward facing step flow was adopted to the numerical simulation. The velocity-vorticity formulation for the incompressible Navier-Stokes equation was used to solve the flow problems. In numerical model, explicit Adams-Bashforth scheme was proposed to solve the Helmholtz vorticity transport equation. The Fast Fourier Transform (FFT) was suggested to directly solve the velocity Poisson's equation. In conjunction with the staggered grid system, the boundary condition of vorticity is satisfied automatically and without any consideration. Iteration process is not necessary in the solving process between velocity and vorticity of proposed numerical method. By the way, the numerical solution reaches second-order accuracy in both time and space. The steady solution of 3D backward-facing step flow for different Reynolds numbers was obtained from the numerical computation. The computational results were agreeable with the experimental data. This proves that the numerical scheme is very powerful to solve the three dimensional incompressible flow problems.

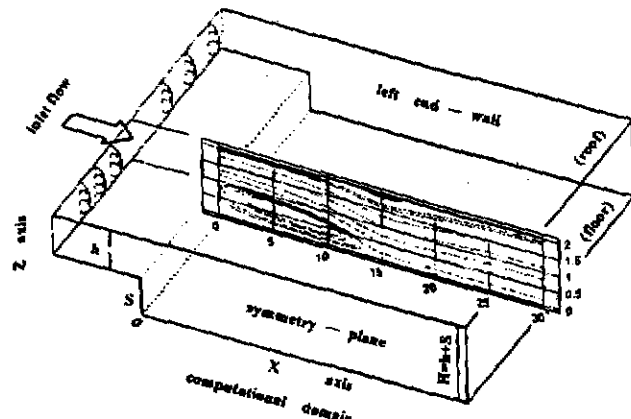
**KEYWORDS:** velocity-vorticity, three-dimensional flows, backward-facing step flow, Helmboltz equation, Poisson equation.



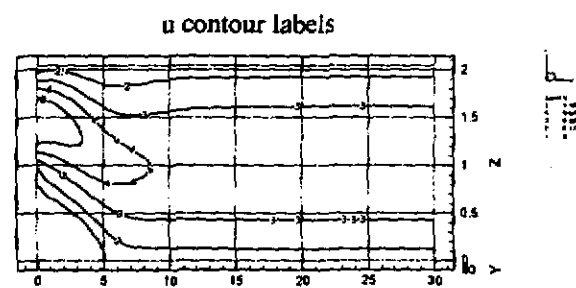
圖一、三維流場變數及網格配置圖



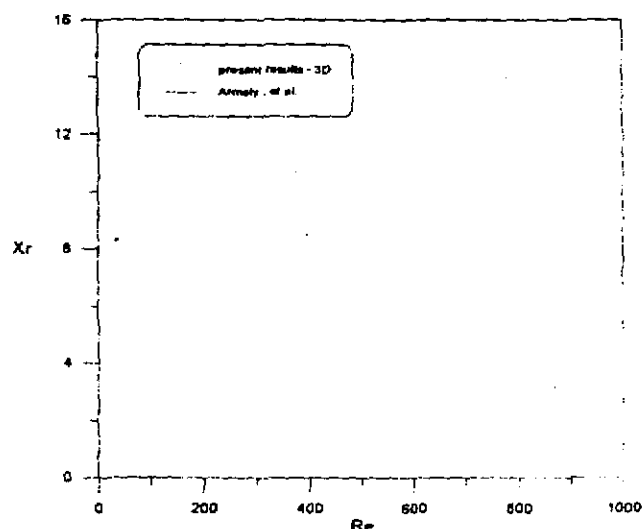
圖二、三維後向階梯流流場示意圖



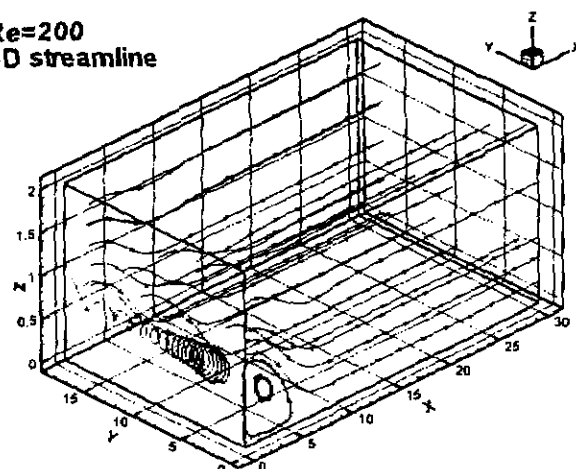
圖三、再接觸長度 $X_r$ 與雷諾數關係之實驗與數值  
模式比較圖



圖四、 $Re=200$ ，二維流線及速度 $u$ 之等值線圖



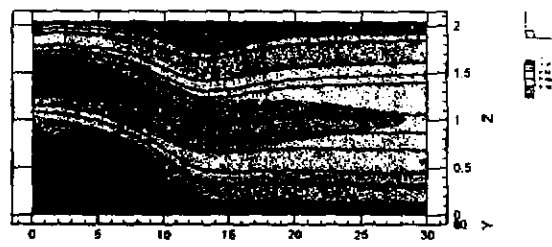
圖五、 $Re=200$ ，三維流線圖



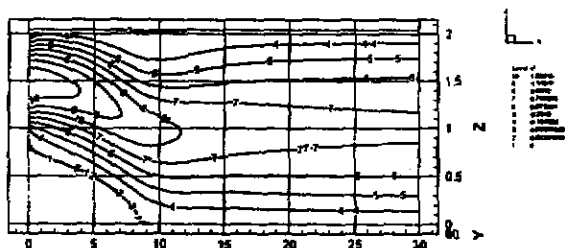
2D streamline and  $u$  contour



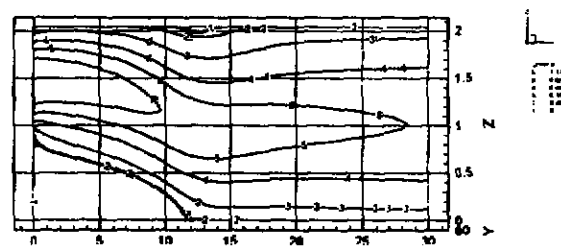
2D streamline and  $u$  contour



$u$  contour labels



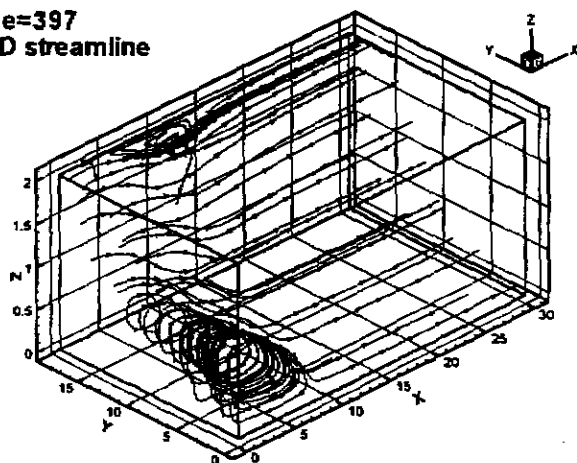
$u$  contour labels



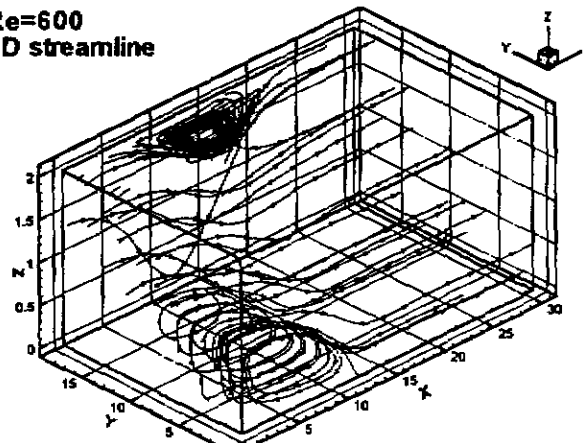
圖六、 $Re=397$ ，二維流線及速度 $u$ 之及等值線圖

圖八、 $Re=600$ ，二維流線及速度 $u$ 之及等值線圖

$Re=397$   
3D streamline



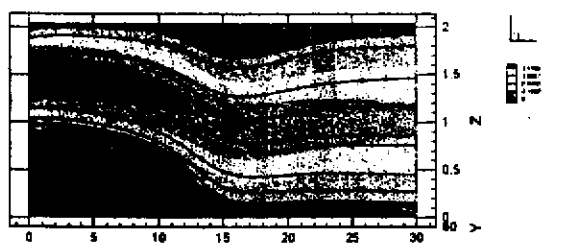
$Re=600$   
3D streamline



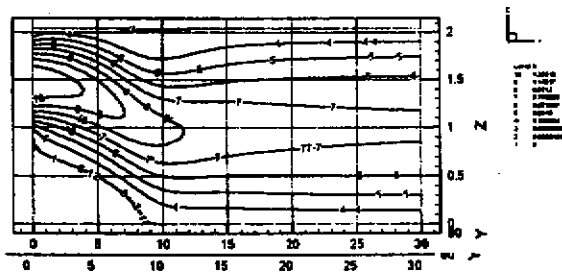
圖七、 $Re=397$ ，三維流線圖

圖九、 $Re=600$ ，三維流線圖

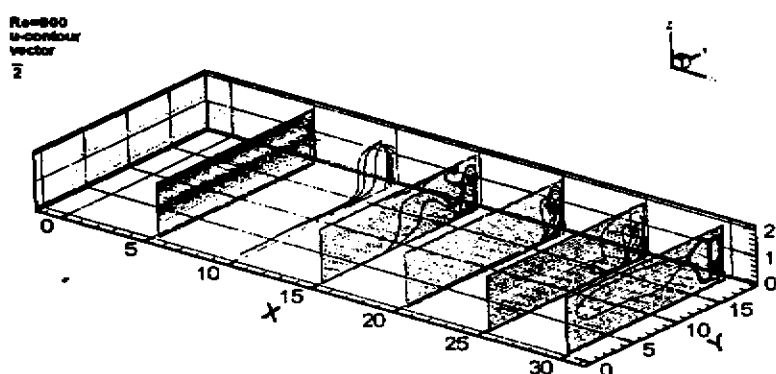
2D streamline and u contour



u contour labels



圖十、 $Re=800$ ，二維流線及速度u之及等值線圖



圖十一、 $Re=800$ ，三維速度向量及u之等值線圖

B7. Eldho, T.L., and Dr. Young, D.L., 2000, "Solution of the Velocity-vorticity Navier-Stokes Equations using Dual Reciprocity Boundary Element Method", CD-ROM Proceedings of 14<sup>th</sup> Engineering Mechanics Conference, ASCE, Austin, Texas, 2000.

Fourteenth

卷之三

IES Conference

四

四庫全書

卷之三

卷之三

卷之三

卷之三

二三

三

卷之三

*Engineering Mechanics 2000, Int. Conference, ASCE, May 2000, Texas, USA*

**Solution of the Velocity-Vorticity Navier-Stokes Equations  
Using Dual Reciprocity Boundary Element Method**

**T. I. Eldho, D.L. Young**

*Department of Civil Engineering & Hydrotech Research Institute*

*National Taiwan University, Taipei, Taiwan 10617*

*Email: eldho@hy.ntu.edu.tw; dlyoung@hy.ntu.edu.tw*

**SUMMARY**

This paper describes the use of dual reciprocity boundary element method (DRBEM) for the solution of incompressible viscous flow problems using velocity-vorticity variables. The model involves the solution of vorticity transport equation for vorticity whose solenoidal vorticity components are obtained by solving Poisson equations involving the velocity and vorticity components. Both the Poisson equations and the vorticity transport equation are solved iteratively using DRBEM and combined to determine the velocity and vorticity vectors. Here the results of 2-dimensional Navier-Stokes problems with low Reynolds number in a typical cavity flow are obtained and compared with other models. The DRBEM model has been found to be satisfactory.

**KEY WORDS**

Navier-Stokes equations, velocity-vorticity, dual reciprocity boundary element method

**1. INTRODUCTION**

For the solution of incompressible viscous flow problems, the velocity-vorticity form of Navier-Stokes equations has been established as an effective formulation. The main advantage of this formulation includes the numerical separation of the kinematic and kinetic aspects of the fluid flow from the pressure computation, which is determined afterwards from the known velocity and vorticity fields. Boundary Element Method (BEM) has been established as a powerful numerical tool in the solution of various fluid flow problems (Power and Wrobel, 1995). The main advantages of BEM are: reduction in computational dimensions, easiness in discretization and data preparation and direct solution to flux term at the boundaries. The major problems in using the general BEM techniques to solve the incompressible viscous flows are the difficulties in dealing with the convective and time dependent terms unless internal cells are defined (Brebbia et al. 1984).

Dual reciprocity boundary element method (DRBEM) employs a fundamental solution corresponding to a simpler equation and treat the remaining terms, through a procedure which involve a series expansion using global approximating functions and the applications of the reciprocity principle (Partridge et. al, 1992) so that a boundary only solution is possible.

To solve the incompressible viscous flow problems, here DRBEM is used. In the DRBEM solution of Navier-Stokes equations, the fundamental solution of Laplace equation is used. The vorticity boundary conditions are got by the DRBEM solution of the Poisson equations. An iterative scheme is used to solve the system of equations after the numerical discretization by DRBEM. The feasibility of the DRBEM model has been demonstrated using the model problem of flow in a driven square cavity.

## 2. GOVERNING EQUATIONS

For two-dimensional incompressible viscous flow problems, if  $(u, v)$  are the velocity vectors ( $\bar{u}$ ) and  $\omega$  is the corresponding vorticity, the governing Navier-Stokes equations in the velocity-vorticity formulation can be written as:

$$\frac{\partial \omega}{\partial t} + \bar{u} \cdot \nabla \omega = \frac{1}{Re} \nabla^2 \omega \quad (1)$$

$$\nabla^2 u = -\frac{\partial \omega}{\partial y}; \quad \nabla^2 v = \frac{\partial \omega}{\partial x} \quad (2)$$

The vorticity vector  $\bar{\omega}$  can be expressed as,  $\bar{\omega} = \nabla \times \bar{u}$ . A solution is sought in the domain satisfying the initial conditions,  $\bar{u} = \bar{u}_0$ ,  $\bar{\omega} = \nabla \times \bar{u}_0$  at initial time and the boundary conditions,  $\bar{u} = \bar{u}_r$ ;  $\bar{\omega} = (\nabla \times \bar{u})|_r$  at  $t \geq 0$ .

The solution of vorticity-transport equation (1), in combination with the velocity Poisson equations (2), with reference to initial and boundary conditions, gives the velocity and vorticity distribution all over the domain at the concerned time step.

## 3. NUMERICAL FORMULATION

### 3.1. DRBEM Formulation of Velocity Poisson Equations

Consider the Poisson type velocity equation in  $u$  and  $\omega$ , say

$$\nabla^2 u = -\frac{\partial \omega}{\partial y} = b \quad (3)$$

with velocity boundary conditions as,  $u = \bar{u}_0$  on  $\Gamma_1$ ;  $\bar{q} = \partial \bar{u}_0 / \partial n$  on  $\Gamma_2$ , where  $n$  is the unit outward normal vector. Here, an iterative algorithm is used such that the right hand side of equation (3) is known from the previous step by solving (1).

Solution to equation (3) can be expressed as the sum of the solution of a homogeneous Laplace equation ( $\tilde{u}$ ) and a particular solution ( $\hat{u}$ ) as,  $u = \tilde{u} + \hat{u}$ , such that,  $\nabla^2 \hat{u} = b$ . The DRBEM proposes the use of a series of particular solution  $\hat{u}_j$  instead of a single  $\hat{u}$ . The number of  $\hat{u}_j$  used is equal to the total number ( $N+L$ ,  $N$ = boundary nodes,  $L$ = internal nodes) of nodes in the problem. Following approximation of  $b$  is then proposed,

$$b \approx \sum_{j=1}^{N+L} \alpha_j f_j \approx \sum_{j=1}^{N+L} \alpha_j \nabla^2 \hat{u}_j, \quad (4)$$

where the  $\alpha_j$ - are a set of initially unknown coefficients and the  $f_j$  are approximating function which is geometrically dependent. Using (4) in (3) gives,

$$\nabla^2 u = \sum_{j=1}^{N+L} \alpha_j (\nabla^2 \hat{u}_j) \quad (5)$$

The procedure for developing the boundary element method for the Laplace equation (Brebbia et al., 1984) will now be applied. Equation (5) can be multiplied by the fundamental solution  $u^*$  (for 2-D problems  $u^* = \ln r/(2\pi)$ ), where  $r$  is the distance from the collocation point ( $k$ ) to other field points ( $i$ ) and integrating over the domain producing,

$$\int_{\Omega} (\nabla^2 u) u^* d\Omega = \sum_{j=1}^{N+L} \alpha_j \int_{\Omega} (\nabla^2 \hat{u}_j) u^* d\Omega \quad (6)$$

Applying Green's second identity, (Brebbia et al. 1984) produces the following integral equation for each source node  $i$ ,

$$C_i u_i + \int_{\Gamma} q^* u d\Gamma - \int_{\Gamma} u^* q d\Gamma = \sum_{j=1}^{N+L} \alpha_j \left( C_i \hat{u}_j + \int_{\Gamma} q^* \hat{u}_j d\Gamma - \int_{\Gamma} u^* \hat{q}_j d\Gamma \right) \quad (7)$$

where  $C_i$  is the Green's constant,  $\hat{q}_j = \partial \hat{u}_j / \partial n$  and  $q^* = \partial u^* / \partial n$ . Note that equation (7) involves no domain integrals. The source term  $b$  in (3) has been substituted by equivalent boundary integrals. After introducing the interpolation functions and integrating over each boundary element, the above equation can be

written in the discretized matrix form as:

$$C_i u_i + \sum_{k=1}^N H_{ik} u_k - \sum_{k=1}^N G_{ik} q_k = \sum_{j=1}^{N+L} \alpha_j \left( C_j \hat{u}_j + \sum_{k=1}^N H_{jk} \hat{u}_k - \sum_{k=1}^N G_{jk} \hat{q}_k \right) \quad (8)$$

Applying to all boundary nodes using a collocation technique, and each of the vector  $\hat{u}_j$  and  $\hat{q}_j$  is considered to be one column of the matrices  $\hat{U}$  and  $\hat{Q}$  respectively, equation (8) can be expressed in matrix form as,

$$H u - G q = (H \hat{U} - G \hat{Q}) \alpha \quad (9)$$

Equation (9) is the basis for the application of the DRBEM and involves discretization of the boundary only. Internal nodes may be defined in the number and the location desired by the user. From equation (3), taking the value of  $b$  at  $(N+L)$  points and expressing in a matrix form,  $b = F \alpha$ ;  $\alpha = F^{-1} b$ , where each column of  $F$  consists of vectors  $f_j$  containing the values of the function  $f_j$  at the  $(N+L)$  collocation points. Thus the right hand side vector of (9) is a known vector. Applying the boundary conditions to (9) gives a linear system of equations which are solved using Gauss elimination scheme to get the boundary unknowns. After finding the boundary unknowns, the internal values can be found from equation (9).

The particular solution  $\hat{u}$ , its normal derivative and the corresponding approximating function  $f$  used in DRBEM analysis are limited by the formulation except that the resulting  $F$  matrix, should be non-singular. Here the  $f$  function used is:  $f = 1 + r + r^2 + \dots + r^m$ . Correspondingly,

$$\hat{u} = \frac{r^2}{6} + \frac{r^3}{12} + \dots + \frac{r^{m+2}}{(m+2)^2 + (m+2)}; \hat{q} = \left( r_x \frac{\partial x}{\partial n} + r_y \frac{\partial y}{\partial n} \right) \left( \frac{1}{3} + \frac{r}{4} + \dots + \frac{r^m}{m+3} \right) \quad (10)$$

Other than the boundary only solution, the main advantage of using DRBEM in the solution of the velocity Poisson equations is the exact determination of the vorticity boundary conditions which are obtained as the velocity normal derivative from the solution of (9) together with the no-slip boundary conditions.

### 3.2. DRBEM Formulation of Vorticity Transport Equation

Consider the advection-diffusion type vorticity transport equation (1),

$$\nabla^2 \omega = R_s \left( \frac{\partial \omega}{\partial t} + \bar{u} \cdot \nabla \omega \right) = R_s b(x, y, \omega, t) \quad (11)$$

As mentioned earlier, an iterative procedure is used to solve equation (11). In the current iteration it will be assumed that the values of  $(u, v)$  are known from the previous iteration. The fundamental solution of Laplace equation is used in the solution (11). Appropriate boundary conditions  $\omega$  or  $q (\partial \omega / \partial n)$  and initial conditions should be prescribed.

As in section 3.1, using the DRBEM, solution to equation (11) can be expressed as the sum of the solution of a homogeneous Laplace equation  $\tilde{\omega}$  and a particular solution  $\hat{\omega}$  as,  $\omega = \tilde{\omega} + \hat{\omega}$  such that,  $\nabla^2 \hat{\omega} = b$ . The DRBEM proposes the use of a series of  $N+L$  particular solution  $\hat{\omega}_j$ . Following approximation of  $b$  is then proposed,

$$b \approx \sum_{j=1}^{N+L} \alpha_j f_j \quad (12)$$

where the  $\alpha_j$  are a set of initially unknown coefficients and the  $f_j$  are approximating function. As explained in section 3.1, we can finally write equation (12) as:

$$\nabla^2 \omega = R_s \sum_{j=1}^{N+L} \alpha_j (\nabla^2 \hat{\omega}_j) \quad (13)$$

Similar to the procedure in section 3.1, using the 2D fundamental solution of Laplace equation in  $r/(2\pi)$ , using the BEM procedure and after the boundary discretization and integration, the final system of equations in matrix form is obtained as:

$$H \omega - G q = R_s (H \hat{\omega} - G \hat{Q}) \alpha \quad (14)$$

Similar in section 3.1,  $b = F \alpha$  or  $\alpha = F^{-1} b$  and putting  $S = -(H \hat{\omega} - G \hat{Q}) F^{-1}$  and substituting for b, equation (14) can be written as:

$$H \omega - G q = S \left[ R_s \left( \frac{\partial \omega}{\partial t} + u \frac{\partial \omega}{\partial x} + v \frac{\partial \omega}{\partial y} \right) \right] \quad (15)$$

Setting,  $\omega = F \beta$  or  $\beta = F^{-1} \omega$ . Differentiating  $\omega$  with respect to x and y,

$$\frac{\partial \omega}{\partial x} = \frac{\partial F}{\partial x} F^{-1} \omega; \frac{\partial \omega}{\partial y} = \frac{\partial F}{\partial y} F^{-1} \omega \quad (16)$$

Therefore equation (15) can be written as,

$$H \omega - G q = R_s S \left[ \frac{\partial \omega}{\partial t} + \left( u \frac{\partial F}{\partial x} + v \frac{\partial F}{\partial y} \right) F^{-1} \omega \right] \quad (17)$$

Putting  $\omega' = \partial \omega / \partial t$ ;  $E = u \partial F / \partial x + v \partial F / \partial y$ , we can write equation (17) as,

$$H \omega - G q = R_s S [\omega' + E F^{-1} \omega] \quad (18)$$

Now substituting,  $M = R_s S E F^{-1}$ ;  $N = -R_s S$ , we can write the final system as:

$$N \omega' + (H - M) \omega = G q \quad (19)$$

Using a two level time integration for  $\omega$  and q and a difference scheme for  $\omega'$

$$\omega = (1 - \theta_u) \omega^m + \theta_u \omega^{m+1}; q = (1 - \theta_q) q^m + \theta_q q^{m+1}; \omega' = \frac{1}{\Delta t} (\omega^{m+1} - \omega^m) \quad (20)$$

where  $\theta_u$  and  $\theta_q$  are weighting factors which position the values of u and q, respectively, between time levels m and m+1. Substituting (20) into (19) gives:

$$\left( \frac{N}{\Delta t} + \theta_u (H - M) \right) \omega^{m+1} - \theta_u G q^{m+1} = \left[ \frac{N}{\Delta t} - (1 - \theta_u) (H - M) \right] \omega^m + (1 - \theta_u) G q^m \quad (21)$$

The right hand side of (21) is known at time  $(m+1) \Delta t$ , since it involves values which have been specified as initial conditions or calculated previously. Upon imposing the boundary conditions at time  $(m+1) \Delta t$ , we can form a linear system, which are solved using the Gauss elimination scheme to find the unknown function values initially over the boundary and then at the internal nodes considered. The approximating functions 'f' given in section 3.1 and corresponding particular solutions and derivatives given in equation (10) are used here also. Here an iterative scheme is used and the derivatives of the vorticity  $\omega$  in x- and y- direction are determined using (16) before the velocity Poisson equations are solved.

#### 4. MODEL RESULTS AND DISCUSSIONS

The proposed DRBEM model has been applied on the classical 'driven flow in a square cavity' problem for which many numerical model results are available in literature. Present model results are compared with a series solution, FDM, FEM and BEM models in 2-D.

The model problem consists of a square cavity with a moving top lid with constant velocity, totally filled with an incompressible viscous fluid. The flow inside the cavity is initially at rest. No slip and impermeability conditions were imposed on all walls, with the velocity at the upper wall set equal to unity. Due to the computational limitations (we used an IBM Pentium II PC with 64 MB RAM), the present analysis is limited to a maximum of computational mesh points of 21x21 (on the boundary and internal nodes). One analysis is presented here, for a Reynolds number of 100.

Figures 1 and 2 show the u and v velocity profiles along the vertical and horizontal centerlines of the cavity, respectively. The velocity variations are compared with a series solution of Burgraff (1966), FDM solution of Ghia et al. (1982), FEM solution of Young and Lin (1986) and BEM solution of Young et al. (2000). The results mostly agree with all the model results, considering the coarse nature of the mesh used in the present analysis. Figure 3 shows the vorticity distribution along the domain and Fig. 4 shows the

velocity vector field.

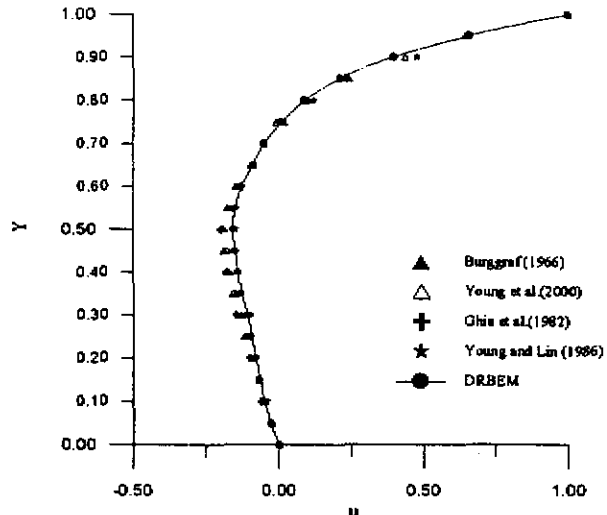


Fig. 1.  $u$ - velocity profile along vertical centerline for  $Re=100$

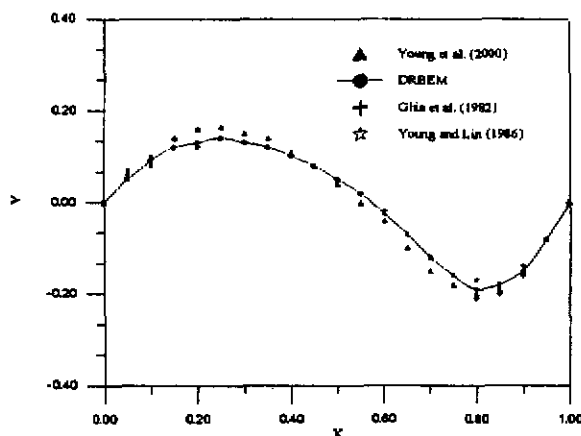


Fig. 2.  $v$ - velocity profile along horizontal centerline for  $Re=100$

DRBEM has been proved to be a feasible method to solve advective-diffusion equation like vorticity transport equation. The necessary vorticity boundary conditions are determined by the DRBEM solution of the velocity Poisson equations together with the no-slip boundary conditions. Hence the present model in which the velocity Poisson equations and vorticity transport equation are solved using DRBEM, and the iterative scheme combining both models provides the best way to treat the velocity-vorticity formulation for two-dimensional incompressible viscous flow problems.

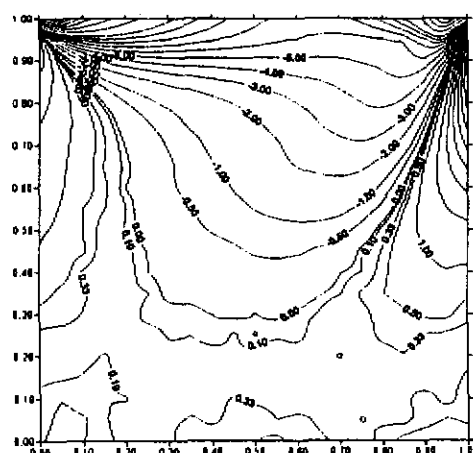


Fig. 3. Vorticity distribution for  $Re=100$

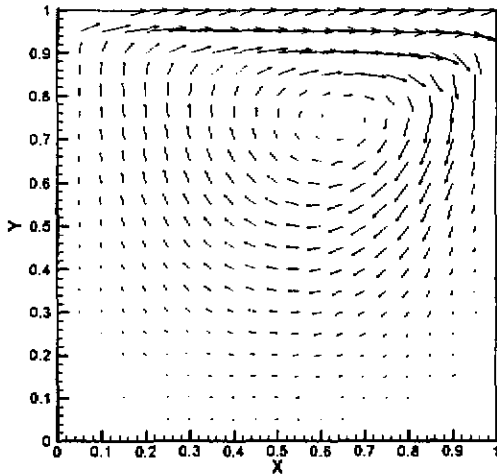


Fig. 4. Profile of the flow vectors for  $Re=100$

## 5. CONCLUDING REMARKS

Here a dual reciprocity boundary element method for solving the velocity-vorticity Navier-Stokes equations is presented. The Poisson type velocity equations and the vorticity transport equation are solved using DRBEM. The vorticity boundary conditions for the solution of vorticity transport equation are exactly obtained from the DRBEM solution of velocity Poisson equations. The use of DRBEM enables one to have a boundary only solution for the problem. Here the results of 2-D Navier-Stokes problems with low Reynolds number in a typical square cavity are presented. A comparison with other models demonstrates the feasibility of the DRBEM model.

## ACKNOWLEDGEMENTS

The work reported in this paper was supported by the National Science Council of Taiwan. It is greatly appreciated.

## REFERENCES

- Brebbia, C.A., Telles, J.C.F., and Wrobel, L.C. (1984). *Boundary Element Techniques Theory and Applications in Engineering*. Springer-Verlag, Berlin.
- Burgraff, O.R. (1966). Analytic and numerical studies of structure of steady separated flows. *J. Fluid Mech.* 24, 131-151.
- Ghia, U., Ghia, K.N., Shin, C.T. (1982) High-Re solutions for incompressible flow using the Navier-Stokes equations and a multigrid method. *J. Comput. Phys.* 48, 387-411.
- Partridge, P.W., Brebbia, C.A., and Wrobel, L.C.(1992). *The Dual Reciprocity Boundary Element Method*, Computational Mechanics Publications, Southampton.
- Power, H., Wrobel, L.C.(1995) *Boundary Integral Methods in Fluid Mechanics*. Computational Mechanics Publications, Southampton.
- Young, D.L., Lin, Q.H. (1986) Application of finite element method to 2-D flows. *Proc. 3rd National Conf. On Hydraulic Engineering*, Taipei, pp.223-242.
- Young, D.L., Yang, S.K., Eldho T.I. (2000). The solution of the Navier-Stokes equations in velocity-vorticity form using Eulerian-Lagrangian boundary element method. *Int. J. Numer. Meth. Fluids* (in press).

B8. Lo, D.C., and Young, D.L., 2000, "Two-dimensional Velocity-vorticity Formulation of the Incompressible Flows by Finite Element Method", Proceedings of 7<sup>th</sup> National Computational Fluid Dynamics Conference, Kenting, 2000, pp.F-1-F-8.

## Two-Dimensional Velocity-Vorticity Formulation For The Incompressible Flows By Finite Element Method

Der-Chang Lo/Graduate student  
Department of Civil Engineering & Hydrotech Research Institute  
National Taiwan University  
Taipei, Taiwan, R.O.C

Der-Liang Young/professor

in this study, the motion of incompressible viscous fluid in a two-dimensional domain is solved by the finite element method using the velocity-vorticity formulation. To demonstrate the model feasibility, first of all the steady Stokes flow in a square cavity are computed. The results of square cavity flow are comparable with the numerical solutions of Burggraff(1966,FDM) and Yang(1997,BEM). Then the unsteady Navier-Stokes flow are computed and compared with other models. The results reveal that finite element analysis is a very powerful approach in the realm of computational fluid mechanics.

include the explicit method, implicit methods, and fully-implicit method. The difference between these methods is that if we use explicit method, it has the strict limitation of the time,  $\Delta t$ . On the other hand, if the implicit method is used, although the range of  $\Delta t$  is not restricted, it is suitable to use smaller value of  $\Delta t$  to ensure that at the high Reynolds number, each iterative steps can guarantee the convergence of the iterative solution.

### Abstract

**Keywords:** Velocity-Vorticity formulation, Finite Element Method, Navier-Stokes equations, square cavity flow

### 1. Introduction

Finite element method (FEM) has been proved to be very convenient and most promising for obtaining spatial approximation to problems with complex geometries. Finite element theory provides an effective methodology for construction of discrete and/or semi-discrete approximations to variational boundary value problems in computational mechanics, including the different forms of the Navier-Stokes equations in fluid mechanics. Three formulation are well known for the solution of the incompressible Navier-Stokes equations, in terms of : primitive variables of pressure and velocity, velocity-stream function and velocity-vorticity. The first two formulations have been thoroughly investigated by various researchers for two dimensional and three dimensional problems using various numerical methods such as finite difference (FDM), finite element (FEM) and boundary element methods (BEM). The third formulation in terms of velocity and vorticity also has been explained in the last decade, mainly in two dimensions using various numerical schemes.

In the computational methodology of unsteady incompressible viscous fluid flows, the fractional step methods have been proven to be effective. However semi-implicit FEM methods have gained some advantages of stability and simplicity. Different time marching methods to solve the vorticity transport equation are another feature in this study. The schemes

### 2. GOVERNING EQUATIONS

The partial differential equation set governing viscous, laminar flow of an incompressible fluid is a subject class of the familiar nonlinear Navier-Stokes system. Let  $\Omega$  be the fluid domain, which is surrounded by a piecewise smooth boundary  $\Gamma$ . By using vector form, the corresponding basic equation of conservation of mass, momentum are

Continuity

$$\nabla \cdot \bar{u} = 0 \quad (1)$$

Momentum

$$\frac{\partial \bar{u}}{\partial t} + \bar{u} \cdot \nabla \bar{u} = -\nabla p + \frac{1}{Re} \nabla^2 \bar{u} \quad (2)$$

where  $\bar{u}$  is the velocity vector,  $p$  is the pressure,  $Re$  is the Reynolds number and  $t$  is the time. Equation (1) and (2) represent the Navier-Stokes equations in the pressure-velocity formulation.

The vorticity vector  $\bar{\omega}$  can be expressed as:

$$\bar{\omega} = \nabla \times \bar{u} \quad (3)$$

By taking the curl of both sides of Eq. (2) and using Eqs. (1) and (3), we can obtain the vorticity transport equation as:

$$\frac{\partial \vec{\omega}}{\partial t} + \vec{u} \cdot \nabla \vec{\omega} = \vec{\omega} \cdot \nabla \vec{u} + \frac{1}{Re} \nabla^2 \vec{\omega} \quad (4)$$

By taking the curl of Eq. (3) and using Eq. (1) we get,

$$\nabla^2 \vec{u} = -\nabla \times \vec{\omega} \quad (5)$$

which is vector form of Poisson equation for  $\vec{u}$ .

Equation (4) and (5) with  $\vec{u}(u, v)$  as velocity and  $\vec{\omega}(\omega_x, \omega_y, \omega_z)$  as vorticity vectors are known as Velocity-Vorticity formulation of the Navier-Stokes equations and can replace Eqs. (1) and (2) in which  $\vec{u}$  and  $p$  are variables.

The two-dimensional velocity-vorticity formulation for the incompressible flows can be derived from the Eqs. (4) and (5) as:

$$\frac{\partial \omega}{\partial t} + u \frac{\partial \omega}{\partial x} + v \frac{\partial \omega}{\partial y} = \frac{1}{Re} \nabla^2 \omega \quad (6)$$

$$\nabla^2 u = -\frac{\partial \omega}{\partial y} \quad (7)$$

$$\nabla^2 v = \frac{\partial \omega}{\partial x} \quad (8)$$

For Navier-Stokes equations, the solution of vorticity transport equation in Eq. (6), in combination with the velocity Poisson equations, (7) and (8), gives the velocity and vorticity distribution all over the domain at the concerned time step.

We seek a solution in the domain  $\Omega$  which satisfies the initial conditions,

$$u = u_0, v = v_0, \omega = \omega_0 \quad \text{at } t=0 \quad (9)$$

no-slip boundary conditions of velocity on the boundary  $\Gamma$  of  $\Omega$ .

As far as vorticity boundary condition is concerned, it is not known a prior. From the Stokes theorem, the vorticity boundary conditions can be written as,

$$\omega = \frac{1}{area} \oint \vec{u} \cdot d\vec{s} \quad (10)$$

### 3. FINITE ELEMENT FORMULATION

The arbitrary element velocity and vorticity are approximated as ( By using indicial notation and summation convention for repeated indices )

$$\omega_j = N_j \omega_j \quad (11)$$

$$u_j = N_j u_j \quad (12)$$

$$v_j = N_j v_j \quad (13)$$

where  $N_j$  denotes the interpolation or shape function of vorticity and velocity. The weak formulations of equation (6), is obtained by using the standard Galerkin method

$$0 = \iint N_i \left( \frac{\partial \omega}{\partial t} + u \frac{\partial \omega}{\partial x} + v \frac{\partial \omega}{\partial y} - \frac{1}{Re} \left( \frac{\partial^2 \omega}{\partial x^2} + \frac{\partial^2 \omega}{\partial y^2} \right) \right) d\Omega \quad (14)$$

and using a time integration for the time derivative of  $\omega$ , Eq.(14) can be written as,

$$0 = \sum \iint N_i N_j \frac{d\omega}{dt} d\Omega + \sum \iint (N_k u_k N_i \frac{\partial N_j}{\partial x} + N_k v_k N_i \frac{\partial N_j}{\partial y}) \omega_j \cdot d\Omega - \sum_{S'} \int q_n N_i d\Gamma + \frac{1}{Re} \sum \iint \left( \frac{\partial N_i}{\partial x} \frac{\partial N_j}{\partial x} + \frac{\partial N_i}{\partial y} \frac{\partial N_j}{\partial y} \right) \omega_j d\Omega \quad (15)$$

$$\text{where } q_n = \frac{\partial \omega}{\partial x} n_x + \frac{\partial \omega}{\partial y} n_y$$

For two dimension , if  $q_n = 0$  or  $\omega$  is specified on the boundary, then the surface integration vanishes. Equation (15) can be written in the form,

$$\sum [M_{ij}^e] \left[ \dot{\omega}_j \right] + [L_{ij}^e] [\omega_j] + \frac{1}{Re} [K_{ij}^e] [\omega_j] = \{0\} \quad (16)$$

where

$$M_{ij}^e = \iint N_i N_j d\Omega$$

$$L_{ij}^e = \iint \left( N_k u_k N_i \frac{\partial N_j}{\partial x} + N_k v_k N_i \frac{\partial N_j}{\partial y} \right) d\Omega$$

$$K_{ij}^e = \iint \left( \frac{\partial N_i}{\partial x} \frac{\partial N_j}{\partial x} + \frac{\partial N_i}{\partial y} \frac{\partial N_j}{\partial y} \right) d\Omega$$

$$\omega = \frac{\omega^{n+1} - \omega^n}{\Delta t} \quad (17)$$

The fractional step methods have been proven to be effective, in the meantime semi-implicit FEM method has rendered some advantages of stability and simplicity.

So the Eq.(17) can be written

$$\begin{aligned} & \left\{ \frac{1}{\Delta t} [M_{ij}^{(s)}] + \theta \left[ L_{ij}^{(s)} + \frac{1}{Re} K_{ij}^{(s)} \right] \right\} \{\omega_j\}_{n+1} \\ & = \left\{ \frac{1}{\Delta t} [M_{ij}^{(s)}] - (1-\theta) \left[ L_{ij}^{(s)} + \frac{1}{Re} K_{ij}^{(s)} \right] \right\} \{\omega_j\}_n \end{aligned} \quad (18)$$

Equation (18) confirms that the needed additional data are integration time-step size  $\Delta t$ , implicit factor  $\theta$ , the known data  $\{\omega\}_n$  at any time  $t^n$ .

$\theta = 0$  means explicit method (always instability)

$\theta = 1$  means fully-implicit method

In this model, We add value of  $\theta = \frac{2}{3}$

Consider the Poisson type velocity equation in  $u$  and assuming that the vorticity and its derivatives are known, Eq(7) can be written as follows:

$$\nabla^2 u = b \quad (19)$$

using the method of weighted residuals and Galerkin criterion, Eq. (19) can be written as,

$$0 = \iint N_i \left( \frac{\partial^2 u}{\partial x^2} + \frac{\partial^2 u}{\partial y^2} - b \right) d\Omega \quad (20)$$

$$\Rightarrow 0 = \sum \iint \left( \frac{\partial N_i}{\partial x} \frac{\partial N_j}{\partial x} + \frac{\partial N_i}{\partial y} \frac{\partial N_j}{\partial y} \right) d\Omega + \sum \iint b(N_i N_j) d\Omega \quad (21)$$

### 3. SOLUTION PROCEDURE

Here an iterative scheme is used in the solution of the velocity-vorticity formulation of Navier-Stokes equations. In most of the incompressible viscous flow problems, the most natural boundary conditions arise when the velocity is prescribed all over the boundaries of the problem. The vorticity boundary conditions are originated from the Stokes theorem. In the present model, the velocity poisson equations are initially solved to get the vorticity boundary condition which are used in the solution of the vorticity transport equations. The solution procedure adopted here includes the following iterative steps :

1. Initial condition: Let  $\omega = 0$
2. Solve the velocity Poisson Eqs using FEM
  - a. Calculate the velocity distribution and velocity derivatives at all nodal points
  - b. Determine the new vorticity boundary values
3. Solved the vorticity transport equations
  - a. Get the unknown vorticity values through out the domain
  - b. Calculate the derivatives of the vorticity to be used in the velocity Poisson equation
4. Check for the convergence of the velocity and vorticity components in the present iteration. If convergence criterion is satisfied, then stop and proceed to the next time step, otherwise go to step 2.
5. In the successive time step, use the velocity and vorticity components from the previous time step as initial conditions and use the iterative procedure, steps 2 to 4. The procedure is repeated until the prescribed time step is reached. (Fig 1)

### 5. NUMERICAL EXAMPLE

The aim of workshop is to compute a two-dimensional lid-driven cavity flow(see Fig. 2). The model problem consists of a square cavity of size 1:1 (dimensionless) with a moving top lid with constant velocity of unity (dimensionless) in the x-direction, totally filled with an incompressible viscous fluid. Fig 2 shows the geometry and boundary conditions of the problem.

In the Navier-Stokes system of equations, the intensity of the nonlinearity and the convective effects, are known to be related with the magnitude of the Reynolds number. Therefore, the computational effort required for its numerical solution increases as the Reynolds number increases. An important consequence of this dependency is that the accuracy of the numerical solution, at different values of the Reynolds number, is strongly associated with the way in which the mesh discretisation is defined, requiring a higher density in the regions near the contours, where the boundary layer is developed, as the Reynolds number increases.

For high Reynolds numbers, the use of a coarse mesh often yields a convergent solution without physical meaning. By refining the computational mesh, it is possible to improve the solution of the flow phenomena, but at the expense of increasing the computational cost. In the present examples, use of a non-uniform mesh (Fig 3.) is better than uniform mesh to solve the Navier-Stokes equations.

**Re=0**

The case presented here, is for steady state Stokes flow conditions ( $Re = 0$ ). Figure 4(a) shows the velocity profiles for  $Re = 0$  on vertical and horizontal centerlines. The results are compared with Burggraf (1966) and Young(1997)et. The streamlines and velocity vector are shown Fig4(b), 4(c). The distribution of vorticity contour is shown in Fig4(d).

**Re=100**

In Figure 5(a), we plot the velocity filed, and the

vertical and horizontal centre-line velocity profiles, respectively, obtained with the present approach without the use of the domain decomposition scheme for the case of  $Re=100$ . In this case, we used  $81 \times 81$  nodes. As can be observed, for this small value of the Reynolds number, the results based upon a velocity-vorticity formulation are in close agreement with the benchmark values obtained by Burggraf (1966) and Ghia (1982) et al., using a finite difference multigrid numerical scheme. As pointed out previously, as the flow regions near the corners, the flow contains singularities associated with infinite values of the velocity and surface traction. The distribution of velocity, streamlines, and vorticity contours are shown in figure 5(b), 5(c), 5(d).

#### Re=1000

When  $Re$  is increased, the inertia begins to play an important role. As a consequence, the vortex center has shifted downstream, vorticity distribution get more complex, and corner eddies start to appear. As shown in Fig. 6(a) to 6(d) which illustrates the velocity profiles, velocity distribution, streamlines and vorticity contours.

As  $Re$  increase to 1000, the above-mentioned physical characteristics become more conspicuous. In particular, the vortex center first moves downstream, and finally moves back to the geometric center of the cavity. This illustrates the fact that viscous forces is confined only to the boundary layer, and most of the region away from the boundaries behaves like the inviscid core of a vortex, as mentioned by Burggraf (1966).

The formation of corner eddies, as pointed out by Moffatt (1964) is another very strange phenomenon in the square cavity simulation. It is seen that the nonlinearity (high  $Re$ ) and corner separation are two major mechanisms to form the secondary currents. There appear a big lower right-hand secondary eddy and a small lower left-hand secondary eddy.

#### Re=5000

As  $Re$  increases further, the number of secondary eddies will increase. It is observed that as many as five secondary eddies will be formed in the upper left, lower right, and lower left corners when  $Re$  approaches 5000. This also indicates that the inertia force is another trigger factor in the formation of secondary eddies. Fig 7(a), 7(b), 7(c) illustrates the transformation of vorticity in the cavity flow. Fig. 7(d), 7(e) shows the distribution of streamlines and velocity of a recirculating flow at  $Re=5000$ .

Table 1 provides a summary of the preliminary results of the high  $Re$  over accomplished with respect to each scheme. In addition, some authoritative literature in this effort is also included for comparison. It is better to compute high Reynolds number by using velocity-vorticity formulation from the results.

## 6. CONCLUDING REMARK

Finite element method model has been developed for solving the velocity-vorticity Navier-Stokes equations

in two dimensions. Here the results of low Reynolds number to high Reynolds number problems, in a typical cavity flow are presented and compared with other numerical models. Computational results show that the FEM presented here provides an efficient method for numerical investigation of two-dimensional incompressible viscous fluid in motion.

## ACKNOWLEDGEMENTS

The work reported in this paper was supported by the National science council, the Republic of China, under the grant of NSC 87-2611-E-002-031. It is greatly appreciated.

## REFERENCES

Batcher, G.K., *Fluid Dynamics*, Cambridge University Press, 1967

Burggraf, O.R., *Analytic and Numerical Studies of Structure of Steady Separated Flow*, J. Fluid Mech., 24 pp. 113-151, 1966

Gustafson, K., and Halasi K., *Vortex Dynamics of Cavity Flows*, J. Comput. Phys., 64, pp. 279-319, 1986

Hwu T.Y., Young D.L., Chen Y.Y., *Chaotic Advections for Stokes Flows in Circular Cavity*, J. Engineering Mech., August, pp. 774-782, 1997

Liggett, J. A., *Fluid Mechanics*, McGraw-Hill, Inc., 1994

Lugt H.J., *Vortex Flow in Nature and Technology*, John Wiley and Sons, Inc. 1983

Napolitano M., and Pascazio G., *A Numerical Method for the Vorticity-Velocity Navier-Stokes Equations in Two and Three Dimensions*, Comput. Fluids, 19, pp. 489-495, 1991

Burnett, D. S., 1987, *Finite element analysis: from concepts to applications*, Addison-Wesley Pub. Co.

Comini, G., Manzan, M., and Cortella, G., 1997, *Open boundary conditions for the streamfunction-vorticity formulation of unsteady laminar convection*, Numerical Heat Transfer, Part B, 31, 217-234

楊德良、楊勝凱，使用速度-渦度變數及邊界積分法求解二維穩態非壓縮Stokes流場，第二十屆全國力學會議論文集(一)，pp.422-429，1996

廖清標、許正元、賴仲凱，利用速度-渦度列式法求解不可壓縮流，第四屆全國計算流體力學研討會論文集，pp.73-82，1997

劉英宏，利用速度-渦度法解析三維黏性不可壓縮場，國立台灣大學土木工程學研究所碩士論文，199

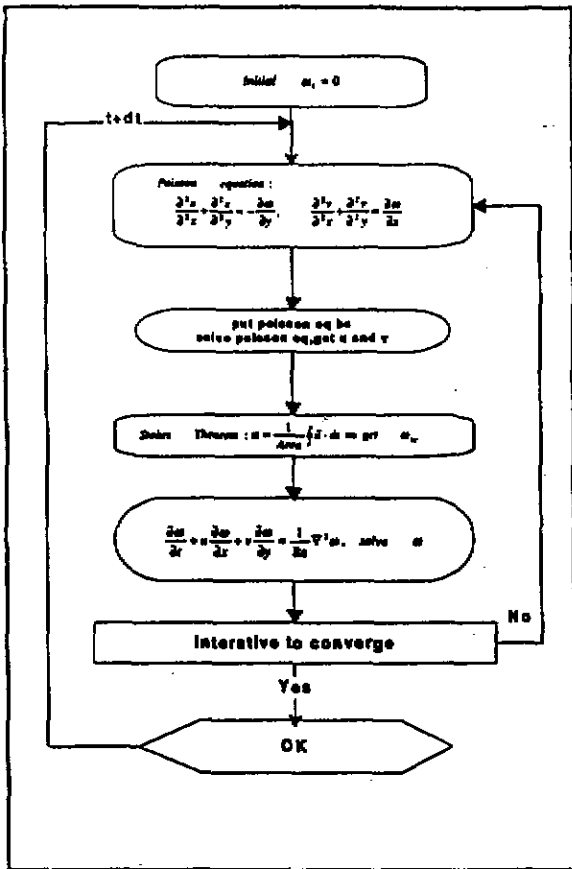


Fig 1: Flow chart for Velocity-Vorticity

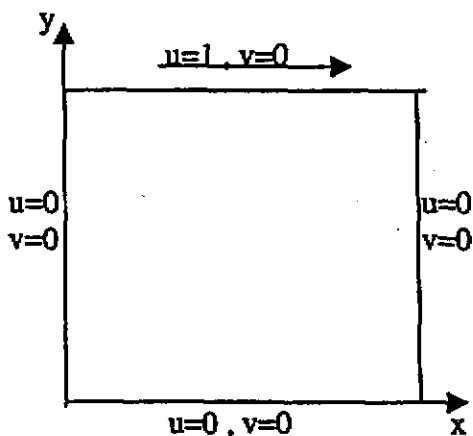


Fig 2: Model problem with boundary conditions

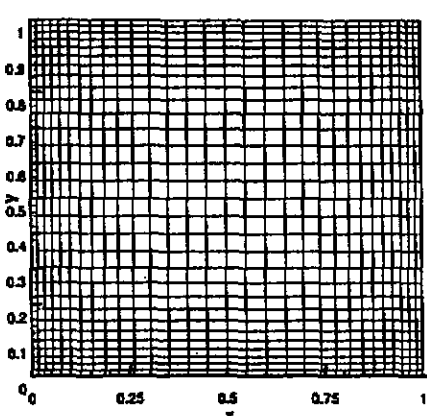


Fig 3: Non-uniform mesh

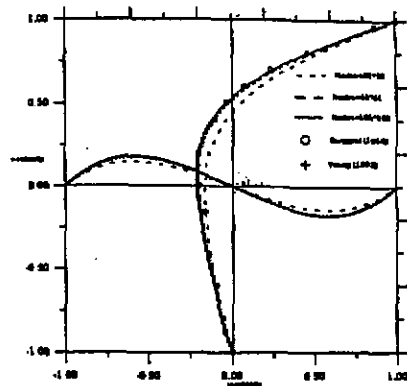


Fig 4(a): Velocity profiles for  $Re=0$  on vertical and horizontal centerlines

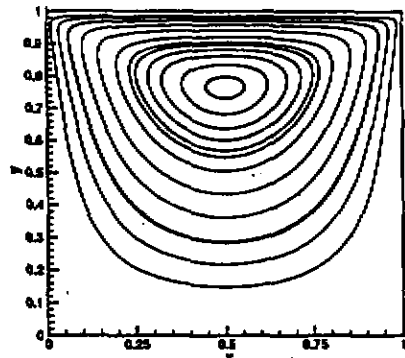


Fig 4(b): Streamlines for  $Re=0$

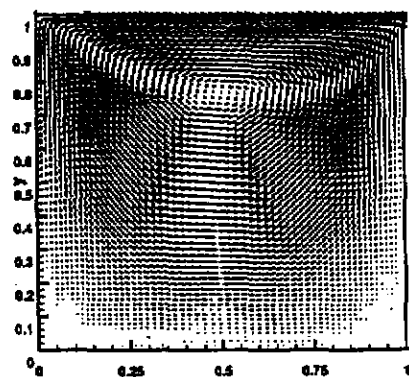


Figure 4(c) Velocity distribution for  $Re=0$

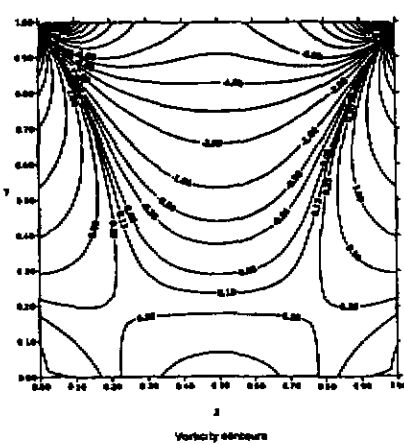


Figure 4(d) Vorticity contours for  $Re=0$

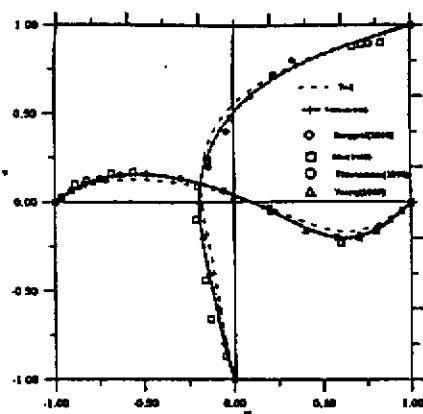


Fig 5(a): Velocity profiles for  $Re=100$  on vertical and horizontal centerlines

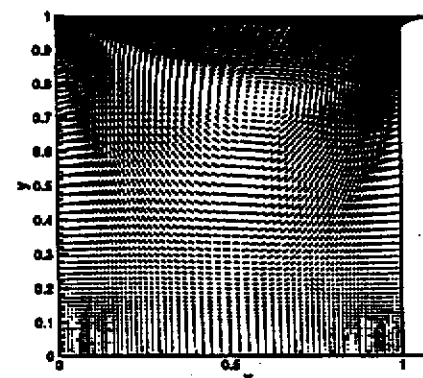


Fig 5(b): Velocity distribution for  $Re=100$

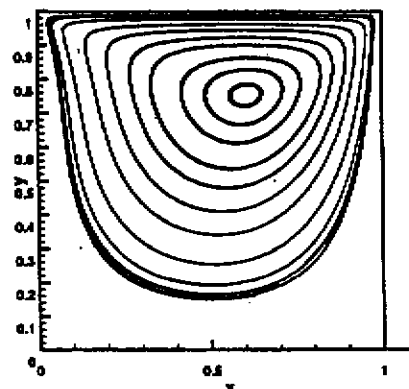


Fig 5(c): Streamlines for  $Re=100$

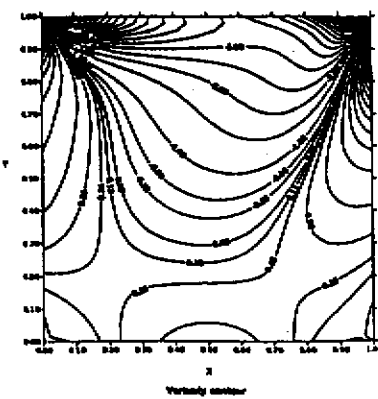


Fig 5(d): Vorticity contour for  $Re=100$

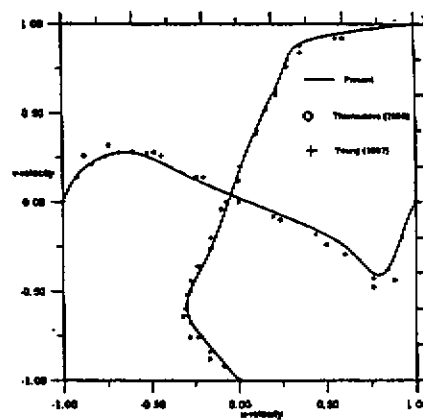


Fig 6(a): Velocity profiles for  $Re=1000$  on vertical and horizontal centerlines

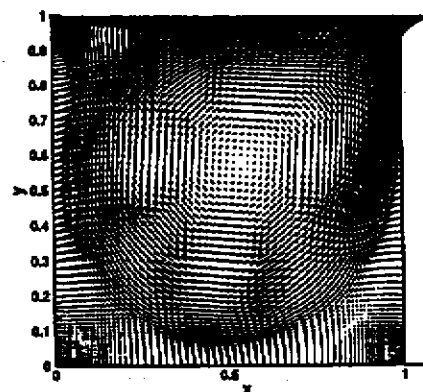


Fig 6(b): Velocity distribution for  $Re=1000$

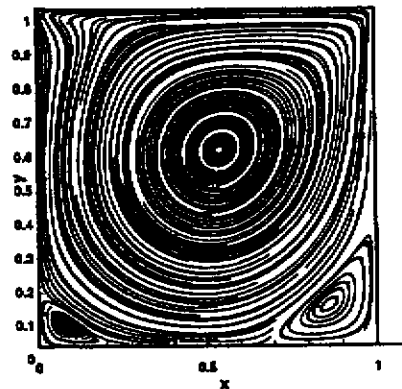


Fig 6(c): Streamline for  $Re=1000$

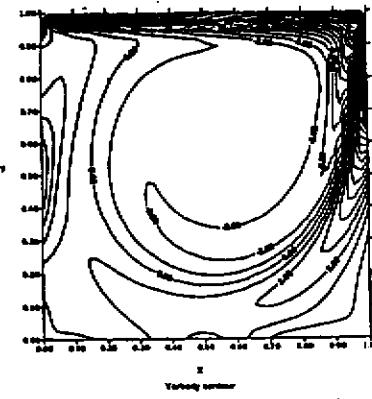


Fig 6(d): Vorticity contour for  $Re=1000$

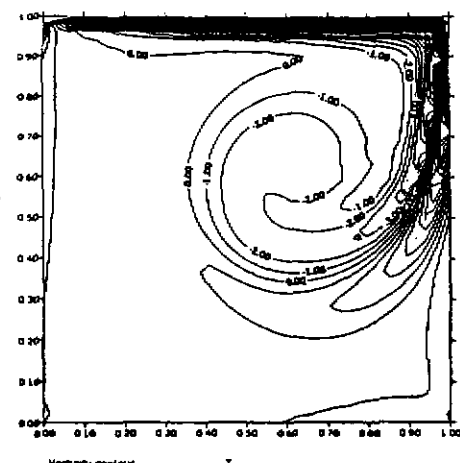


Fig 7(a): Vorticity contour for  $Re=5000(t=10)$

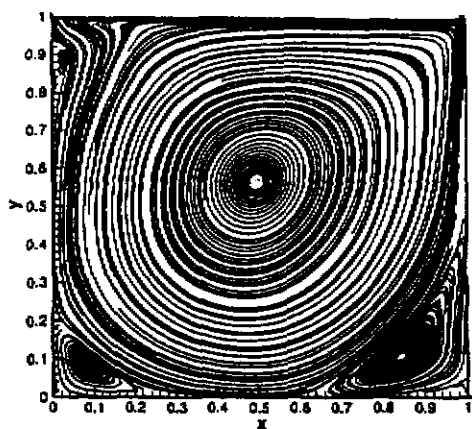


Fig 7(d): Streamline for  $Re=5000(t=80)$

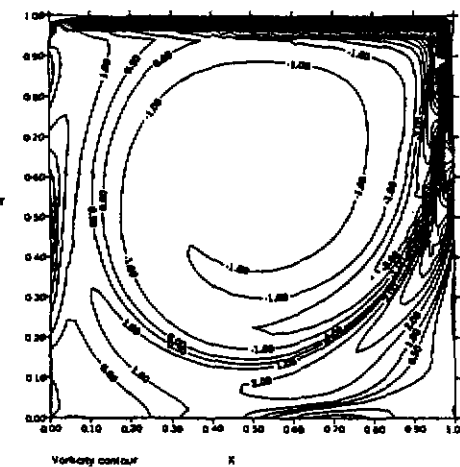


Fig 7(b): Vorticity contour for  $Re=5000(t=20)$

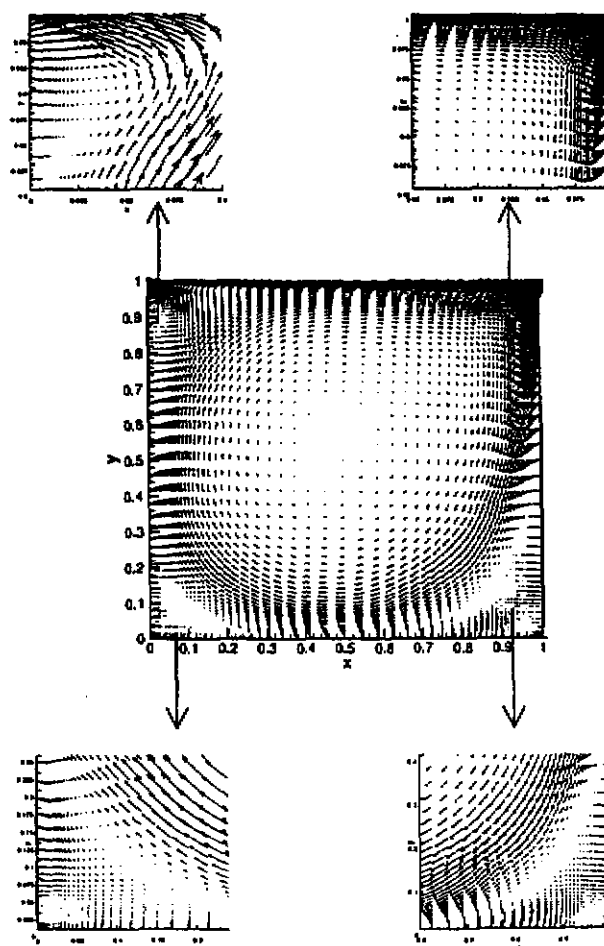


Fig 7(e): Velocity distribution for  $Re=5000$

Fig 7(c): Vorticity contour for  $Re=5000(t=80)$

Table 1 : Comparision of primary vortex, streamline with others for square cavity

Reynolds no	Reference	Year	Mesh size	Method	$\varphi_c$	$a_t$	Location	Circulation	Continuity
Re=0	Burggraf	1966	40*40	D	-0.1	-3.2	(0.5,0.76)		
	Yang	1997	100*4	L	-0.1002	-3.148	(0.5,0.76)	-1.01399	8.9E-15
	Present	2000	201*201	Ts	-0.0998	-3.21	(0.5,0.76)	-0.990	-1.03E-05
Re=1	Young	1997	60*4	L	-0.0931	-3.021	(0.483,0.767)	-0.96199	-4.5E-14
	Liao	1997	32*32	D	-0.09955	-3.21377	(0.5,0.766)		
	Present	2000	81*81	Ts	-0.0941	-3.161	(0.5,0.767)	-0.9561	-2.3E-05
Re=100	Burggraf	1966	40*40	D	-0.1015	-3.14	(0.62,0.740)		
	Ghia	1982	129*129	D	-0.1034	-3.1665	(0.617,0.734)		
	Yang	1997	60*4	L	-0.098	-3.018	(0.583,0.75)	-0.96325	4.2E-14
	Liao	1997	32*32	D	-0.1012	-3.251	(0.629,0.747)		
	Present	2000	81*81	Ts	-0.0978	-3.221	(0.63,0.748)	-0.981	-3.01E-04
Re=200	Yang	1997	60*4	L	-0.96261	-2.734	(0.617,0.717)	-0.96261	1.1E-14
	Liao	1997	32*32	D	-0.1026	-2.608	(0.619,0.69)		
	Present	2000	101*101	Ts	-0.971	-2.74	(0.62,0.72)	-0.9659	4.02E-05
Re=400	Burggraf	1966	40*40	D	-0.1017	-2.142	(0.56,0.610)		
	Ghia	1982	257*257	D	-0.1139	-2.29	(0.555,0.606)		
	Yang	1997	60*4	L	-0.1011	-2.227	(0.583,0.633)	-0.96058	3.7E-14
	Liao	1997	32*32	D	-0.1006	-2.146	(0.566,0.621)		
	Present	2000	101*101	Ts	-0.101	-2.21	(0.578,0.651)	-0.964	3.2E-04
Re=800	Yang	1997	60*4	L	-0.1028	-2.12	(0.55,0.60)	-0.96539	-4.6E-14
	Present	2000	101*101	Ts	-0.1011	-2.10	(0.56,0.60)	-0.9861	6.01E-05
	Ghia	1982	129*129	D	-0.1179	-2.049	(0.531,0.563)		
Re=1000	Young&Lin	1986	16*16	T	-0.1038	-1.6605	(0.535,0.570)		
	Yang	1997	60*4	L	-0.1028	-1.885	(0.55,0.583)	-0.96924	-7.5E-14
	Liao	1997	48*48	D	-0.1032	-1.8502	(0.535,0.574)		
	Present	2000	101*101	Ts	-0.1041	-1.876	(0.53,0.57)	-0.9681	-7.2E-05
	Yang	1997	60*4	L	-0.1033	-1.767	(0.533,0.567)	-0.9556	5.3E-15
Re=2000	Liao	1997	72*72	D	-0.1083	-1.7577	(0.524,0.55)		
	Present	2000	101*101	Ts	-0.1055	-1.761	(0.52,0.56)	-0.987	1.06E-05
	Present	2000	101*101	Ts	-0.1056	-1.746	((0.496,0.53))	-0.9658	-6.1E-06
Re=3200	Liao	1997	128*128	D	-0.1082	-1.6809	(0.516,0.534)		
	Present	2000	121*121	Ts	-0.1091	-1.691	(0.505,0.52)	-0.987	-2.25E-05

T: Triangular Element (FEM)

Ts: Triangular Element (FEM) - Staggered method

D: Finite Difference Method

L:

Linear Element (BEM)

FEM: Finite Element Method

BEM: Boundary Element Method

## 利用速度-渦度與有限元素法求解二維不可壓縮流場

羅德章/研究生 楊德良/教授

台灣大學土木工程學系

## 摘要

本文是利用速度-渦度法與有限元素法來求解二維不可壓縮、黏性流體的運動。為了驗證本模式的正確性，本文首先計算穩態的史托克斯流場，並和 Burggraf (1966) 與楊勝凱 (1997) 等人作一比較。接著，在進行非穩態的奈維爾-史托克斯方程式的計算，所得到的結果和前人的結果也作一比較，由數值結果顯示有限元素法對計算流體力學有著很好的精度。

B9. 楊德慶, 2000, “非線性三維河口污染物擴散模式之研究-速度渦度法(2/3)”,  
第 22 屆海岸工程研討會, 國科會海洋工程學門成果發表會, 高雄市, 2000  
年 11 月。